SUPPLEMENT 7

HONG KONG MEDICAL JOURNAL
Volume 25 Number 5 October 2019

The official publication of the
Hong Kong Academy of Medicine and
the Hong Kong Medical Association

HONG KONG MEDICAL JOURNAL
香港醫學雜誌

Health and Medical Research Fund

Research Dissemination Reports

醫療衞生研究基金

研究成果報告

Cancer
癌症

Infectious Disease
傳染病

Neurology
神經內科

ISSN 1024-2708

香港醫學專科學院出版社
HONG KONG ACADEMY OF MEDICINE PRESS

HONG KONG MEDICAL JOURNAL 香港醫學雜誌
Volume 25 Number 5 October 2019
Supplement 7

HONG KONG MEDICAL JOURNAL 香港醫學雜誌
Volume 25 Number 5 **October 2019**
SUPPLEMENT 7

Health and Medical Research Fund

Research Dissemination Reports

CANCER

INFECTIOUS DISEASE

NEUROLOGY

Editorial

Dissemination reports are concise informative reports of health-related research supported by the Health and Medical Research Fund (and its predecessor funds) administered by the Food and Health Bureau. In this edition, we present 11 dissemination reports of projects related to cancer, infectious diseases, and neurology. In particular, three projects are highlighted due to their potentially significant findings, impact on healthcare delivery and practice, and/or contribution to health policy formulation in Hong Kong.

Oesophageal squamous cell carcinoma (OSCC) is highly metastatic and often fatal. The majority of patients do not survive for more than 1 year after diagnosis. Early detection would allow prompt initiation of treatment, which could save or extend lives. Lung et al[1] aimed to determine if serum amyloid A could be useful as an early biomarker for OSCC. Using genomic and blood samples of more than 220 patients with OSCC, they found that serum amyloid A was 100% sensitivity and 100% specificity for early detection of OSCC, with plasma samples having higher sensitivity and specificity than serum samples.

Every year influenza virus infections are responsible for hundreds of excess deaths and thousands of excess hospitalisations. It is important to differentiate infection incidence from severity. In epidemics, young children usually have higher incidence and elderly people have higher severity. Cowling et al[2] aimed to estimate the age-specific attack rate of influenza A and B in a representative group of households between late 2012 and early 2015 and evaluate the risk factors for influenza virus infection. Over the course of five local influenza epidemics, the overall incidence of infection was about 5% to 11% for influenza A and about 4% for influenza B, with incidence in children being relatively low. Age and chronic diseases were significantly associated with the risk of infection.

As the ageing population increases, the burden from physical and cognitive healthcare needs will increase. Dementia is one of the most devastating and costly diseases facing elderly people and their carers. Wong et al[3] aimed to determine whether foreign language learning (English) was effective in boosting cognitive reserve and promoting healthy cognitive function and whether it was superior to other established cognitively stimulating activities in 137 Cantonese-speaking local elders with mild cognitive impairment. Overall, foreign language training was more effective than music listening in boosting cognitive reserve and promoting health cognitive function, and was more effective than crossword and puzzles in reducing the risk of cognitive deficits and in improving a broad range of cognitive functions.

We hope you will enjoy this selection of research dissemination reports. Electronic copies of these dissemination reports and the corresponding full reports can be downloaded individually from the Research Fund Secretariat website (https://rfs2.fhb.gov.hk/). Researchers interested in the funds administered by the Food and Health Bureau also may visit the website for detailed information about application procedures.

Supplement co-editors

Dr Edmond SK Ma
Chief Scientific Reviewer
(Research Office)
Food and Health Bureau

Dr Richard A. Collins
Senior Scientific Reviewer
(Research Office)
Food and Health Bureau

References

1. Lung HL, Lung ML, Law S. Serum amyloid A1 polymorphisms as risk factors in oesophageal squamous cell carcinoma. Hong Kong Med J 2019;25(Suppl 7):S4-8.
2. Cowling BJ, Peiris JSM, Kwok KO. Influenza virus infections in Hong Kong in 2013-14: a community-based longitudinal seroepidemiological study. Hong Kong Med J 2019;25(Suppl 7):S23-6.
3. Wong PCM, Ou J, Pang CWY, et al. Foreign language learning as potential treatment for mild cognitive impairment. Hong Kong Med J 2019;25(Suppl 7):S41-3.

Serum amyloid A1 polymorphisms as risk factors in oesophageal squamous cell carcinoma

HL Lung *, ML Lung, S Law

KEY MESSAGES

1. Serum amyloid A1 provides 100% sensitivity and 100% specificity for early detection of oesophageal squamous cell carcinoma. The choice of using serum or plasma samples is critical for circulating serum amyloid A detection.
2. The median survival time of patients with serum amyloid A1.3/1.5 genotype was shorter than that of patients with other genotypes (10.63 months vs 20.41 months, P=0.004). This was likely due to the extra high-circulating interleukin 6 concentrations.

Hong Kong Med J 2019;25(Suppl 7):S4-8
HMRF project number: 01120886

[1] HL Lung, [2] ML Lung, [3] S Law

[1] *Department of Biology, Hong Kong Baptist University*
[2] *Department of Clinical Oncology and Centre for Cancer Research, The University of Hong Kong*
[3] *Department of Surgery, The University of Hong Kong*

* Principal applicant and corresponding author: hllung2@hkbu.edu.hk

Introduction

Oesophageal carcinoma is highly metastatic and often fatal. Most such patients do not survive for >1 year after diagnosis, and the 5-year survival rate is <10%. Early detection of oesophageal squamous cell carcinoma (OSCC) is difficult because the symptoms are not obvious until the tumour is advanced and metastatic at the time of presentation. It is essential to identify an early biomarker for this disease.

Serum amyloid A is an acute-phase high-density lipoprotein–associated apolipoprotein, which is dramatically elevated (up to 1000-fold) in serum following injury, inflammation, and cancer. SAA has been used as a cancer biomarker in many tumour types including OSCC.[1] Elevated SAA level is associated with cancer progression and survival. SAA is a generic term for a family of acute-phase proteins encoded by various *SAA* genes with a high genetic variation.

During the acute-phase response, the hepatic biosynthesis of SAA is up-regulated by pro-inflammatory cytokines including interleukin (IL)-1, IL-6, and tumour-necrosis factor.[2] There is SAA induction of different extracellular matrix degradation enzymes such as matrix metallopeptidases (MMPs).[3] SAA plays a role in the modulation of inflammatory and immune responses via inducing MMP-9 in human monocytic cells.[4] Thus, using SAA, IL-6, IL-8, and MMP-9 as serum biomarkers may increase sensitivity and specificity for OSCC detection. We therefore compared their usefulness in OSCC diagnosis and prognosis with a classic tumour biomarker – squamous cell cancer antigen (SCCA). Both plasma and serum samples of OSCC patients were included to examine the protein levels of interest. In addition, we investigated whether particular *SAA1* genotypes are associated with the elevated SAA, IL-6, IL-8, and MMP-9 levels in OSCC patients. In addition, gene expression in OSCC tumour tissues was also assessed. We aimed to determine (1) whether *SAA1* polymorphisms are correlated with the *SAA1* and its related gene expression in the OSCC tumour tissues, and (2) whether *SAA1* polymorphisms have any functional role in OSCC development.

Methods

This study protocol was approved by the Institutional Review Board of The University of Hong Kong / Hospital Authority Hong Kong West Cluster (Ref No. UW 13-393), and written consent was obtained from all patients. A total of 226 patients with OSCC who underwent oesophagectomy with no preoperative chemoradiotherapy between 2000 and 2012 at the Department of Surgery, Queen Mary Hospital were included. The genomic DNA from blood samples of these patients and of 295 healthy controls (supplied by the Hong Kong Red Cross) were collected for SAA1 genotyping.

ELISA was performed to detect circulating proteins in plasma and serum samples of 85 of the OSCC patients and in plasma samples of 100 of the healthy controls. For gene expression analysis, matched non-tumour biopsies and OSCC biopsies (from 60 of the 85 OSCC patients) were used. The gene expression of *SAA1*, *IL-6*, *IL-8*, *MMP-9* was determined by quantitative PCR using previously described methods.[5] SAA1-genotyped OSCC patients, healthy controls, and hospital controls (non-cancer patients in Queen Mary Hospital) were compared in terms of plasma/serum SAA (Abcam), IL-6 (R&D Systems), IL-8 (R&D Systems), MMP-9

(R&D Systems), and SCCA1 (Biomatik). The use of hospital controls was for adjusting confounding factors such as associated chronic inflammatory states. PCR amplification and DNA sequencing were carried out for blood samples of 226 OSCC patients and healthy controls as described.[5]

Associations between pathological variables of OSCC patients and gene and protein expression of *SAA1* were analysed using SigmaPlot (Systat Software) and SPSS (Version 19, IBM, Armonk [NY], USA). The student's *t* test was used unless stated otherwise. A P value of <0.05 was considered statistically significant.

Results

SAA1.1, *1.3*, and *1.5* were the major SAA1 isoforms observed in both OSCC patients and healthy people in Hong Kong. *SAA1.1/1.1*, *SAA1.3/1.3*, *SAA1.5/1.5*, *SAA1.1/1.3*, *SAA1.1/1.5*, and *SAA1.3/1.5* were the six major *SAA1* genotypes (Fig 1). Patients with *SAA1.3/1.5* genotype (n=45) had a shorter median survival time than those with other *SAA1* genotypes (10.63 months vs 20.41 months, P=0.004). The Kaplan-Meier survival analysis confirmed that *SAA1.3/1.5* genotype was associated with worse overall survival, and the longest survival time was observed in patients with the *SAA1.5/1.5* genotype (41.07 months). Thus, the *SAA1.3/1.5* variant was identified as a predictive biomarker of poor survival.

Pre-treatment OSCC patients (n=85) and healthy controls (n=100) were compared in terms of plasma levels of SAA, IL-6, IL-8, and MMP-9, as well as the conventional biomarker SCCA1 level. The plasma SAA level was ~10-fold more in OSCC patients than in healthy controls (536.86 ng/mL vs 50.06 ng/mL, $P=3.38 \times 10^{-59}$, Fig 2). In contrast, the serum levels of SAA and SCCA1 in the same patients were ~7-fold less than the plasma levels of SAA and SCCA1. Compared with hospital controls, OSCC patients only had a 1.43-fold increase in serum SAA (P=0.00083) and no significant elevation of serum levels of SCCA1, IL-6, IL-8, or MMP-9. Patients with high plasma and serum IL-6 levels showed poorer overall survival. High plasma/serum IL-6 levels in *SAA1.3/1.5* patients were likely to contribute to the poor survival of ~20% of OSCC patients (Fig 3).

The sensitivity and specificity of the circulating SAA, IL-6, IL-8, MMP-9, and SCCA1 for OSCC detection at different stages were calculated by

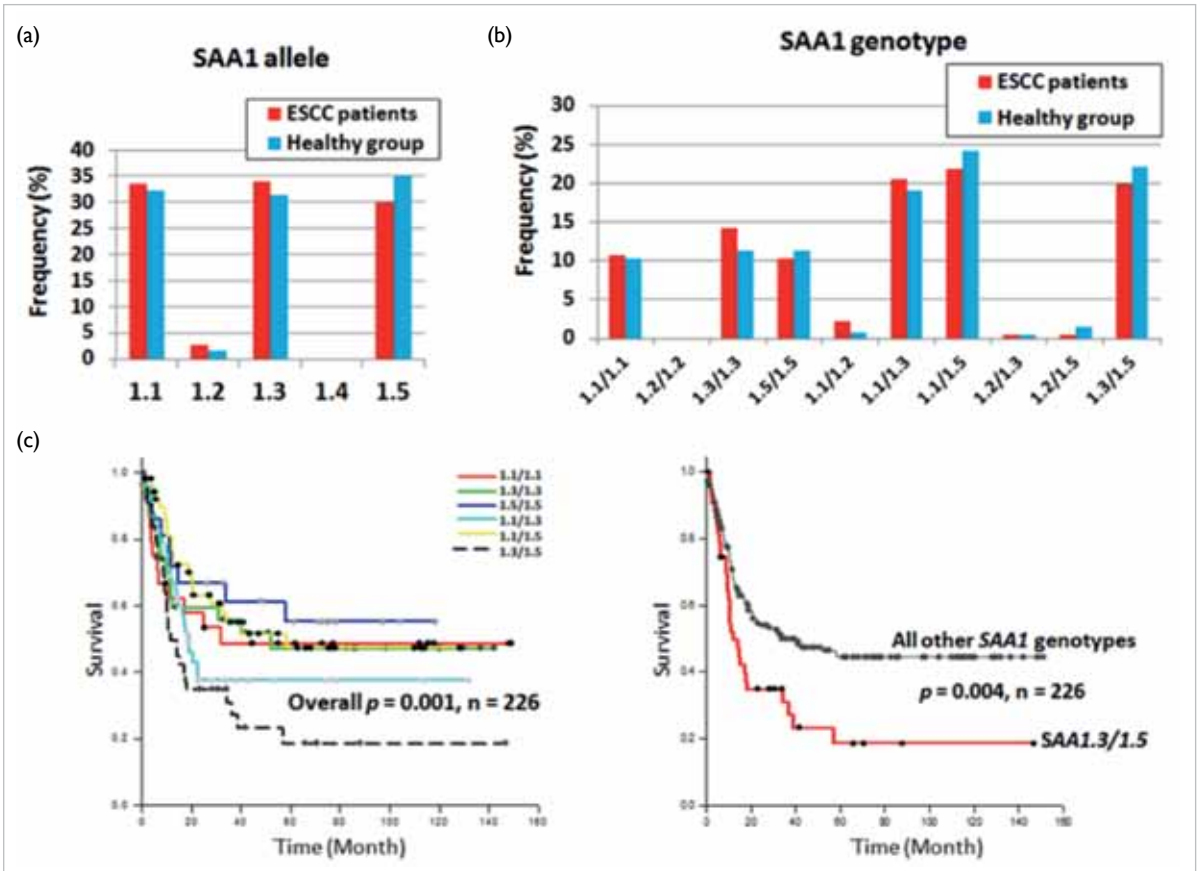

FIG 1. Frequency of (a) *SAA1* alleles and (b) *SAA1* genotypes in patients with oesophageal squamous cell carcinoma (OSCC). (c) The overall survival of patients with different major *SAA1* genotypes and the overall survival of patients with *SAA1.3/1.5* or other five major *SAA1* genotypes.

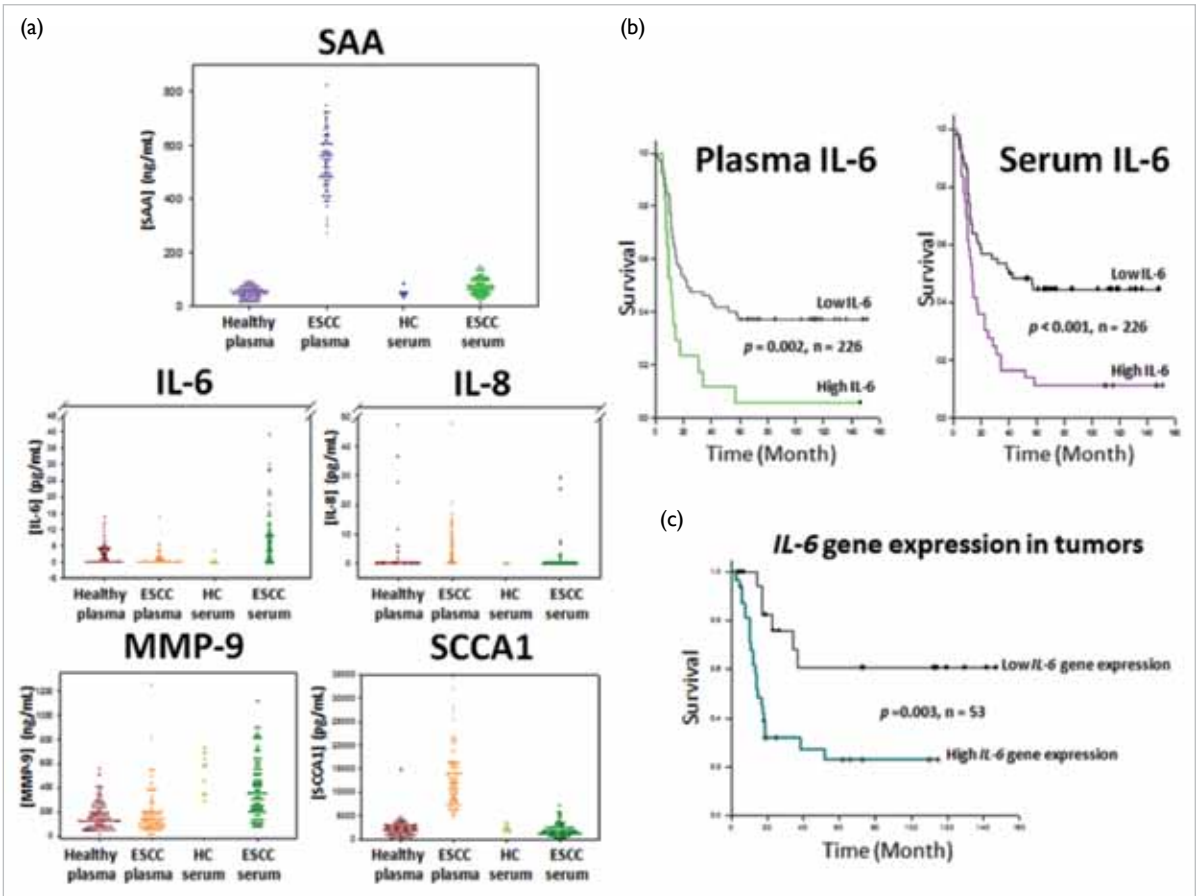

FIG 2. (a) Circulating SAA, IL-6, IL-8, MMP-9, and SCCA1 protein levels in plasma and sera of pre-treatment patients with oesophageal squamous cell carcinoma (OSCC), in plasma of healthy controls, and in sera of hospital controls. (b) Circulating SAA and IL-6 are prognostic markers. (c) Kaplan-Meier analysis showed that high *IL-6* gene expression is a marker for poor prognosis.

comparing the plasma levels of these proteins in OSCC patients and healthy controls. The plasma SAA and SCCA1 levels were elevated ~10-fold ($P=7.34 \times 10^{-20}$) and ~6-fold ($P=7.51 \times 10^{-10}$), respectively, in the early-stage (stages I and II) OSCC patients. Plasma SAA was better than plasma SCCA1 in detecting early-stage OSCC (specificity, 100% vs 99%; sensitivity, 100% vs 100%; area under the receiver operating characteristic curve, 1.00 vs 0.99; Fig 3). The circulating IL-6, IL-8, and MMP-9 had much lower sensitivity and specificity than either the plasma SAA or SCCA1. Thus, plasma SAA alone is an ideal biomarker for early OSCC detection.

Tumours with *SAA1.3/1.5* genotype showed the highest gene expression of *SAA1*, *IL-6*, and *MMP-9* and second highest *IL-8* expression among all major *SAA1* genotypes. The high expression levels of *SAA1* (P=0.011) and *MMP-9* (P=0.0097) was associated with *SAA1* genotype, whereas the high IL-6 gene expression was not associated with *SAA1.3/1.5* genotype (P=0.079). The Kaplan-Meier survival analysis showed that high levels of *IL-6* gene expression were associated with poorer survival (P=0.003). Circulating SAA level and gene expression of *SAA1* were not correlated (r=0.0062, P=0.972). Thus, the liver (rather than the tumour) was the major producer of the circulating SAA protein in OSCC patients.

To study the functional roles of these *SAA1* isoforms in OSCC development, *SAA1.1*, *1.3*, and *1.5* were ectopically expressed in three OSCC cell lines. Tumourigenicity was suppressed by restoration of *SAA1.1* and *SAA1.3*. This is in contrast to the appearance of tumours for the *SAA1.5*-expressing cells. The effects of the three *SAA1* isoforms in OSCC angiogenesis was assessed using the tube-forming ability of human umbilical vein endothelial cell tube formation assay. The *SAA1.5*-expressing cell line could not significantly reduce tube formation (P=0.283), whereas the *SAA1.1* and *SAA1.3* reduced by about 35.4% and 37.93%, respectively, of the human umbilical vein endothelial cell tube formation. The in vivo anti-angiogenic activities of the same *SAA1*-expressing cells were

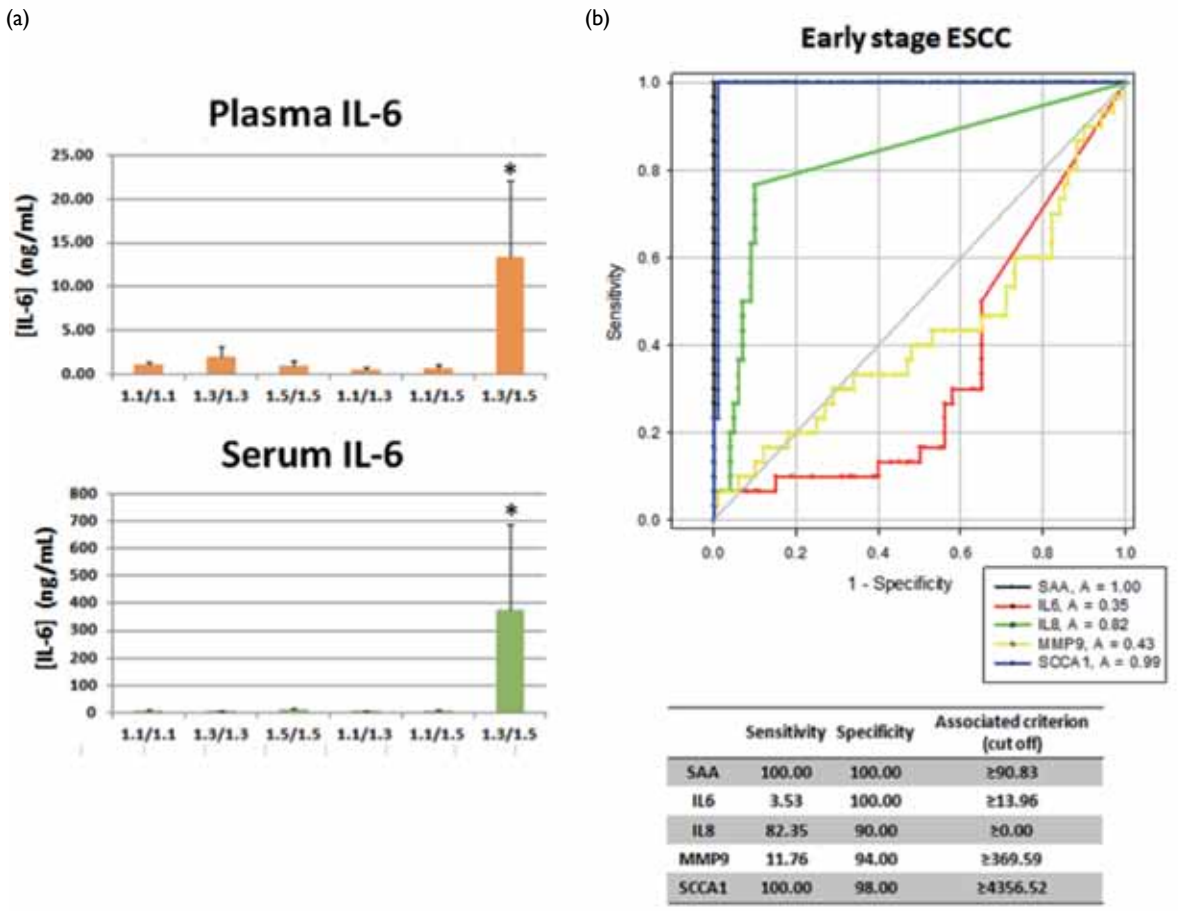

	Sensitivity	Specificity	Associated criterion (cut off)
SAA	100.00	100.00	≥90.83
IL6	3.53	100.00	≥13.96
IL8	82.35	90.00	≥0.00
MMP9	11.76	94.00	≥369.59
SCCA1	100.00	98.00	≥4356.52

FIG 3. (a) Levels of plasma and serum IL-6 in the *SAA1*-genotyped samples. (b) Receiver operating characteristic curves of plasma levels of SAA, IL-6, IL-8, MMP-9, and SCCA1 in detection of early-stage oesophageal squamous cell carcinoma (OSCC).

assessed in mice with the matrigel plug assay. The numbers of microvessels in gel plugs of the *SAA1.1*- and *SAA1.3*-expressing cells reduced by 30.6% and 42.6%, respectively, compared with the vector-alone controls. The number of microvessels of the *SAA1.5*-expressing cells decreased by 8.15%, which was not significant.

Discussion

Plasma SAA is an ideal early detection marker for OSCC. The choice of using plasma or serum samples is critical for the detection of circulating SAA and SCCA1 proteins in cancer patients. Two possible reasons for varying protein levels in plasma and serum are: (1) SAA protein is more stable in plasma with a high protein matrix; and (2) SAA directly interacts with platelets to modulate platelet aggregation, and thus the blood coagulation can sequester most SAA protein in the clotted blood and result in reduced SAA protein in the serum samples. Results of the receiver operating characteristic curve analysis suggest that both plasma SAA and SCCA1 proteins are equally effective for detection of early OSCC. When hospital controls are included, plasma SAA has higher specificity and sensitivity than plasma SCCA1.

OSCC patients with *SAA1.3/1.5* genotype showed the shortest survival time (10.63 months). The abnormal high levels of circulating IL-6, IL-8, and MMP-9 in patients with *SAA1.3/1.5* genotype could be a reason for this short survival time. High-circulating IL-6 was able to stratify poor survival from good survival. Furthermore, the gene expression levels of *SAA1*, *IL-6*, and *MMP-9* were highest in patients with *SAA1.3/1.5* genotypes. Thus, poorer survival outcome was associated with OSCC patients with *SAA1.3/1.5* genotype.

Functional assays for the three *SAA1* variants (*SAA1.1, 1.3, 1.5*) in various OSCC cell lines showed that *SAA1.1* and *1.3* could suppress both tumour formation and angiogenesis, whereas *SAA1.5* had no significant effects. These results suggest that *SAA1.1* and *1.3* have the tumour suppressive function by inhibiting angiogenesis in the primary tumours. The *SAA1.5* seems to encode a defective SAA1 protein in

the anti-angiogenic function.

Acknowledgements

This study was supported by the Health and Medical Research Fund, Food and Health Bureau, Hong Kong SAR Government (#01120886). We thank the Hong Kong Red Cross for providing blood samples from healthy individuals. We also thank Dr Didier Trono for the supply of the lentiviral vectors, pWPI, pMD2.G, and psPAX2.

References

1. Wang JY, Zheng YZ, Yang J, et al. Elevated levels of serum amyloid A indicate poor prognosis in patients with esophageal squamous cell carcinoma. BMC Cancer 2012;12:365.
2. Jensen LE, Whitehead AS. Regulation of serum amyloid A protein expression during the acute-phase response. Biochem J 1998;334:489-503.
3. Migita K, Kawabe Y, Tominaga M, Origuchi T, Aoyagi T, Eguchi K. Serum amyloid A protein induces production of matrix metalloproteinases by human synovial fibroblasts. Lab Invest 1998;78:535-9.
4. Lee HY, Kim MK, Park KS, et al. Serum amyloid A stimulates matrix-metalloproteinase-9 upregulation via formyl peptide receptor like-1-mediated signaling in human monocytic cells. Biochem Biophys Res Commun 2005;330:989-98.
5. Lung HL, Man OY, Yeung MC, et al. SAA1 polymorphisms are associated with variation in antiangiogenic and tumor-suppressive activities in nasopharyngeal carcinoma. Oncogene 2015;34:878-89.

Chinese parental decision making on HPV vaccination for adolescent girls: a longitudinal study

R Fielding *, WWT Lam, JTK Wu, LDL Wang, QY Liao

KEY MESSAGES

1. Descriptive norm beliefs are associated with Chinese parents' intention and planning to vaccinate adolescent daughters against HPV.
2. Anticipation of affective consequences if not vaccinated is a primary motivating factor associated with vaccination intention.
3. A large proportion of Chinese parents hold negative/passive attitudes towards optional vaccines.
4. The government should subsidise HPV vaccination programmes if high coverage is desired.

Hong Kong Med J 2019;25(Suppl 7):S9-12
HMRF project number: 11121501

[1] R Fielding, [1] WWT Lam, [2] JTK Wu, [1] LDL Wang, [1] QY Liao

School of Public Health, The University of Hong Kong:
[1] *Division of Behavioural Health*
[2] *Division of Epidemiology and Biostatistics*

* Principal applicant and corresponding author: fielding@hku.hk

Introduction

HPV vaccination has been available in Hong Kong since 2006. Vaccination decisions for adolescent girls generally devolve to parents. By 2012, only 9% of Hong Kong teenage girls had received HPV vaccination.[1] Most empirical studies on HPV vaccination measured parental knowledge, attitudes, and intention to vaccinate daughters, yet most of these studies did not specify a theoretical framework.[2] Although some studies developed their research questions based on theories, none conducted either model analysis or evaluation of the model fit to predict parental HPV vaccination decision-making. In addition, most studies were cross-sectional and thus reverse causality cannot be ruled out. Therefore, longitudinal studies based on theoretical frameworks are needed to determine how factors that influence parental decision making really translate into adolescent HPV vaccination uptake.

We adopted an extended version of the theory of planned behaviour as the theoretical framework (Fig 1). Parental vaccination intention was assumed to be determined by attitudes towards HPV vaccination, social influence, perceived self- efficacy, and anticipated affective consequence. With interest in the role of additional predictors, we hypothesised that (1) parents who anticipate greater affective consequences have higher vaccination intention; (2) descriptive norms are associated with participants' HPV vaccination intention; and (3) parents with more positive attitudes to general optional vaccines have higher vaccination intention, and in turn predict vaccination planning and vaccination uptake.

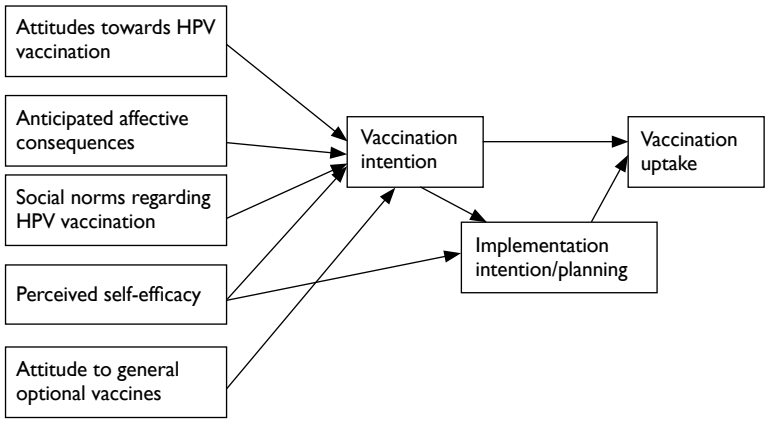

FIG 1. Theory of planned behaviour model for understanding parental decision making on HPV vaccination for their adolescent girls

Methods

A random sample of Hong Kong Chinese parents who had at least one daughter aged 12 to 17 years and were aware of HPV vaccine but have not yet had their daughters vaccinated against HPV were interviewed through telephone about their attitudes and perceptions towards HPV vaccination. At 6 and 12 months after the first interview, the participants were re-contacted to collect their daughters' HPV vaccination status. Structural equation model analysis was used to examine factors predicting adolescent girls' vaccination uptake.

Results

Between February and November 2014, of 3337 eligible parents, 1996 completed the baseline telephone interviews (response rate, 60%). Approximately 40% of the participants regarded optional vaccines as unimportant; 63% considered that it was unnecessary to give their children optional vaccines; 51.9% believed that too many vaccines can harm children's immune systems; and 22.1% said that they would not give their children any vaccines if not mandated by government. Of the 1996 participants, 979 completed and 1017 did not complete the 1-year longitudinal survey; both groups were comparable in terms of sociodemographics (Table).

Of the 1996 participants, 526 (26%) reported that they would 'likely/very likely/certainly' vaccinate their daughter against HPV in the next 6 months. However, at 1-year follow-up survey, among 988 participants who reported their daughters' HPV vaccination status, only 97 (9.8%) of their daughters actually received HPV vaccination.

For structural equation model analysis, only the 988 participants who reported their daughters' HPV vaccination status at 1-year follow-up survey were included. Confirmatory factor analysis assessed the validity and adequacy of the model for each latent variable, leaving six latent variables in the final structural model (Fig 2). Two additional paths were added based on the modification indices, including a path from social norms to vaccination planning and a path from barriers to HPV vaccination to vaccination planning. The paths from perceived self-efficacy to vaccination intention, and from barriers to taking HPV vaccination to vaccination intention were removed. Coefficients for these two paths were non-significant and too small to be meaningful. The final model indicated a good fit, with comparative fit index of 0.95, Tucker-Lewis Index of 0.97, and root

TABLE. Comparison between participants who did (n=979) and did not (n=1017) complete the 1-year follow-up survey

Characteristics	Baseline (n=1996)*	Month 6 (n=1255)*	Month 12 (n=979)*	P value
Age, y	47.5±5.5	47.5±5.5	47.7±5.5	0.789
Sex				0.162
Female	1485 (74.4)	963 (76.7)	742 (75.8)	
Male	511 (25.6)	292 (23.3)	237 (24.2)	
Marital status				0.815
Married	1883 (94.7)	1192 (95.0)	928 (94.8)	
Single/divorced/widowed/separated	106 (5.3)	63 (5.0)	51 (5.2)	
Educational level				0.143
Primary or below	161 (8.1)	87 (6.9)	68 (6.9)	
Secondary	1365 (69.8)	884 (70.4)	685 (70.0)	
Tertiary or above	441 (22.1)	284 (22.6)	226 (23.1)	
Employment status				0.063
Employed	1114 (55.8)	689 (54.9)	530 (54.1)	
Currently unemployed	865 (43.3)	563 (44.9)	448 (45.8)	
Family monthly income, HK$				0.321
<10 000	148 (7.4)	81 (6.5)	72 (7.4)	
10 000 to <20 000	506 (25.4)	324 (25.8)	243 (24.8)	
20 000 to <40 000	575 (28.8)	387 (30.8)	300 (30.6)	
≥40 000	547 (27.4)	372 (29.6)	291 (29.7)	
Birth place				0.276
Hong Kong	1253 (65.1)	807 (64.3)	633 (64.7)	
Mainland China	671 (33.6)	411 (32.7)	318 (32.5)	
Elsewhere	26 (1.3)	34 (2.7)	26 (2.7)	
Religious affiliation	691 (34.6)	426 (33.9)	329 (33.6)	0.885
Children ever experienced vaccination adverse effects	852 (42.7)	546 (43.5)	430 (43.9)	0.146
Health insurance for children	924 (46.3)	597 (47.6)	452 (46.2)	0.837
Family history of cancer	575 (28.8)	398 (31.7)	321 (32.8)	<0.0001

* Data are presented as mean±SD or No. (%) of participants

mean square error of approximation of 0.065.

Parental intention to vaccinate daughters against HPV was greater when perceiving benefits of HPV vaccination (b=0.17), descriptive norms (b=0.28), anticipation of affective consequences (regret/worry) if not vaccinated (b=0.32), and holding positive attitude to general optional vaccines (b=0.09) were all higher. Vaccination planning was associated with barriers to taking HPV vaccination (vaccination cost and concern about potential side-effects of vaccination) [b= -0.31], descriptive norms beliefs (b=0.17), perceived self-efficacy in taking daughter(s) for HPV vaccination (b=0.73), and vaccination intention (b=0.11). Both vaccination intention (b=0.31) and vaccination planning (b=0.18) significantly predict HPV vaccination uptake (Fig 2).

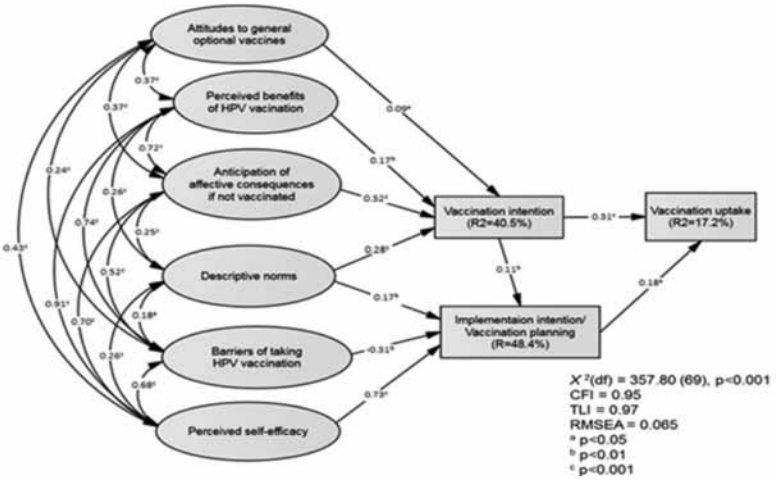

FIG 2. Structural equation model of factors influencing Chinese parents' intention to vaccinate adolescent daughters against HPV and actual vaccination uptake.
Numbers represent the standardised parameters (ß). R2 represents the explained variance of the dependent variables by the predictors (n=988). Ovals represent latent variables; rectangles represent observed variables.

Discussion

The results supported the three hypotheses. Anticipated affective consequences (regret/worry) if not vaccinated was significantly associated with parental HPV vaccination intention, consistent with the utility model prediction that the primary motivating factor for adopting preventive behaviour is resolution of the anxiety associated with the threat, rather than the threat itself.[3] This suggests that vaccination can be both an instrumental- and an emotion-focused coping response to an otherwise uncontrollable threat.[4]

Descriptive norm beliefs were significantly associated with parental vaccination intention and vaccination planning. Parents who perceived that a higher proportion of peers who have vaccinated their daughters also expressed higher intention to vaccinate their daughter. In light of the absence of government-organised HPV vaccination programmes and concrete vaccination advice from healthcare organisations, decision-making regarding HPV vaccination could be difficult owing to uncertainty and ambiguous risks/benefits, and lay responses often revert to reliance on the heuristic of 'imitate the majority'.[5] This results in adoption of the wait-and-see approach, which can impair the value of prophylactic vaccination programmes.

Hong Kong has almost universal immunisation coverage rate for mandatory vaccines, but the uptake rate for optional vaccines is much lower. Some parents considered optional vaccines not important, but Chinese parents accept mandatory vaccines. This may reflect removal of the concerns of cost and side-effects as well as reassurance about efficacy of government-funded vaccination programmes (eg, if government provided the vaccine free-of-charge, they would only do so if it was cost-effective).

Financial cost was a major barrier for HPV vaccination uptake,[1] particularly for disadvantaged families. The median value local Chinese parents willing to pay for the full course of HPV vaccination was HK$1000, which is one third of the market price.[1] A modelling study suggests that among individuals with high conformity to social influence, the vaccination coverage increases only if the vaccination cost is low.[6] Thus, we anticipate that if HPV vaccination cost remains unchanged, and no subsidy is provided, then HPV vaccination coverage will likely continue to be suboptimal in in a high conformity society like Hong Kong.

The theory of planned behaviour posits that intention leads to behaviour, but in this study we observed that although a relatively high proportion (26.4%) of parents expressed positive intention at baseline survey, only 9.8% vaccinated their daughters, indicating that there was a considerable gap between intention and behaviour, with only 21% of those expressing positive intention translating this into action, compared to 14% in those undecided (8.9%) or against vaccination (5%). Barriers to taking HPV vaccination (vaccination cost and concern about potential side effects of vaccination) and perceived self-efficacy were significantly associated with vaccination planning but not vaccination intention, which may partially explain why the actual vaccination rate is much lower than the rate of reported positive intention to vaccinate.

Public health implication/recommendation

Descriptive norms had significant impact on parental HPV vaccination intention. Public health campaigns may utilise social norm marketing to promote HPV vaccination, as behaviour change does not have to start at an individual level. However, it should be

used with caution as normative messages may create a psychological backlash that undermines campaign efforts, and some descriptive norm messages can even induce negative effect. For instance, regarding HPV vaccination for adolescent girls, if the message states that <10% of Hong Kong Chinese girls have been vaccinated against HPV, it may further inhibit parental intention to get their daughter vaccinated. Instead, public health campaigns should use parents as a source of positive messages, eg "Now my daughter has had HPV vaccination, like her friends, I am no longer worried about her risk of developing cervical cancer when she grows up. I feel so much better."

Public health education that emphasises the association between personal lifestyle factors and cancer risk often lacks detailed information about the causes or risk factors for specific cancers (eg, high prevalence of HPV infection in general population). This could result in unintended negative social effects, such as increasing public stigma towards cervical cancer patients. Among many Chinese and western women, cervical cancer is stigmatised as reflecting past promiscuity. Therefore, future cervical cancer prevention programme should emphasise the high prevalence of HPV infection in the general population, which may increase parental awareness/fear of HPV infection and cervical cancer. This may help to reduce optimistic bias and potential stigmatisation towards cervical cancer patients.

Hong Kong Chinese parents consider optional vaccines much less important than mandatory vaccines. Negative attitudes to optional vaccines indicate parental HPV vaccination acceptance and intention. The lack of a formal government-organised HPV vaccination programme encourages parents to adopt a wait-and-see approach, perpetuating low uptake rates. Future public education and campaigns regarding optional vaccines should clarify necessity and provide explicit guidance. If high uptake is required, vaccinations should be free of charge or at very least subsidised. Redesigned vaccination record cards may clarify increasingly complicated combination vaccine regimens. These include both mandatory and optional vaccines, with 'must, should, could' types of recommendation. This would help more parents to make informed decisions and less reliant on herd responses. Increasing the channels for vaccination information delivery, concrete vaccination advice from health professionals, particularly public sector clinicians, and school leaflets, and interactive communications (such as expert-led community-based health education programmes) may facilitate parental acquisition of more accurate and timely information to make informed decisions regarding vaccination.

Financial cost is among the most important barriers to HPV vaccination uptake. Provision of free vaccination for both girls and boys may be considered. Hong Kong government announced to provide 9-valent HPV vaccines free-of-charge to girls of lower income groups who might lack affordable access to this potentially important health initiative. We recommend that offering subsidies for school-based HPV vaccination for all children or, better still, adding HPV vaccine into the mandatory vaccination programme would remove these barriers. A sustained government programme with a move towards a pre-mandatory status, perhaps linked to some financial benefit such as lower health insurance premiums (as with vaccination status) would also prompt increased uptake. Finally, inclusion of the vaccine in the childhood vaccination record, along with other beneficial non-mandatory vaccines would help to reassure parents' need and safety of the HPV vaccine.

Acknowledgements

This study was supported by the Health and Medical Research Fund, Food and Health Bureau, Hong Kong SAR Government (#11121501). The authors would like to thank the participants for their participation and The University of Hong Kong Public Opinion Programme for their assistance in data collection.

Results from this study have been published in:

(1) Wang LD, Lam WW, Fielding R. Hong Kong Chinese parental attitudes towards vaccination and associated socio-demographic disparities. Vaccine 2016;34:1426-9.

(2) Wang LD, Lam WW, Fielding R. Cervical cancer prevention practices through screening and vaccination: a cross-sectional study among Hong Kong Chinese women. Gynecol Oncol 2015;138:311-6.

(3) Wang LD, Lam WWT, Wu J, Fielding R. Psychosocial determinants of Chinese parental HPV vaccination intention for adolescent girls: preventing cervical cancer. Psychooncology 2015;24:1233-40.

References

1. Choi HC, Leung GM, Woo PP, Jit M, Wu JT. Acceptability and uptake of female adolescent HPV vaccination in Hong Kong: a survey of mothers and adolescents. Vaccine 2013;32:78-84.
2. Allen JD, Coronado GD, Williams RS, et al. A systematic review of measures used in studies of human papillomavirus (HPV) vaccine acceptability. Vaccine 2010;28:4027-37.
3. Cohen DR. Utility model of preventive behavior. J Epidemiol Community Health 1984;38:61-5.
4. Lazarus RS, Folkman S. Stress, Appraisal, and Coping. New York: Springer; 1984: 445.
5. Volz KG, Gigerenzer G. Cognitive processes in decisions under risk are not the same as in decisions under uncertainty. Front Neurosci 2012;6:105.
6. Xia S, Liu J. A computational approach to characterizing the impact of social influence on individuals' vaccination decision making. PLoS One 2013;8:e60373.

DNA sequence patterns in human major histocompatibility complex region in southern Chinese

YQ Song *, PS Sham, SP Yip, YH Fan, SY Bao

KEY MESSAGES

1. We developed a programme, quantLD, for genome-wide comparisons of linkage disequilibrium difference between two populations and applied the methods to the major histocompatibility complex region in 1000 Genomes Project phase 3 data. Results suggested that linkage disequilibrium difference exists across populations.
2. We also developed a programme PyHLA for HLA alleles association analysis and applied to a set of 246 APOE ε4 allele negative Alzheimer disease cases and 172 normal controls. HLA-DRB1*07:01 and HLA-C*03 were inversely associated with Alzheimer disease, whereas HLA-DQB1*03:01 and DRB1*09:21 were associated with Alzheimer disease.

Hong Kong Med J 2019;25(Suppl 7):S13-6
HMRF project number: 01121726

[1] YQ Song, [2] PS Sham, [3] SP Yip, [1] YH Fan, [1] SY Bao

[1] *School of Biomedical Sciences, The University of Hong Kong*
[2] *Department of Psychiatry, The University of Hong Kong*
[3] *Department of Health Technology & Informatics, The Hong Kong Polytechnic University*

* Principal applicant and corresponding author: songy@hku.hk

Introduction

The variation LD (varLD) method was developed to assess the extent of differences in linkage disequilibrium (LD) patterns between populations. The varLD method can identify candidate regions with different LD patterns between populations. However, quantification of the difference and how to use the difference to direct the replication and fine mapping of association signals from genome-wide association studies remain unclear.

The major histocompatibility complex (MHC) is a region on chromosome 6 that encodes MHC molecules. In humans, MHC is known as human leukocyte antigen (HLA). The HLA region (3.9 Mb, chromosome 6, 29587512-33516520, NCBI, Build 36.3; 28477797-33448354, GRCh37) contains 224 gene loci, 128 of which are predicted to be expressed.[1] In HLA, there are three major (HLA-A, HLA-B, HLA-C) and three minor (HLA-E, HLA-F, HLA-G) MHC class I genes, and three major (HLA-DP, HLA-DQ, HLA-DR) and two minor (HLA-DM, HLA-DO) MHC class II genes.

Alzheimer disease (AD) is a devastating neurodegenerative disease primarily affecting the elderly people. HLA-DRB1 and HLA-DRB5 alleles were reported as susceptibility loci of AD by genome-wide association study and meta-analysis.

The same disease can be associated with different MHC loci in different populations. An integrated gene map of the extended human MHC has reviewed the MHC genes in relation to paralogy, polymorphism, immune function, and disease.[2] However, the underlying mechanisms of the differences between different populations are poorly understood.

Methods

1000 Genomes Project data

The 1000 Genomes Project phase 3 data were downloaded from the European Bioinformatics Institute (ftp.1000genomes.ebi.ac.uk/vol1/ftp/release/20130502/). This dataset is based on 20130502 sequence freeze and alignments. It contains 2504 individuals from 26 populations. There are 167 082 biallelic variants within the HLA region (human chromosome 6,28,477,797 - 33,448,354 GRCh37). Only 33 722 SNPs with minor allele frequency higher than 1% in all 26 populations were kept for the subsequent analysis.

Quantification of linkage disequilibrium patterns between populations

The programme quantLD (https://github.com/felixfan/quantLD) was developed to measure the LD patterns between populations. The programme takes SNPs genotype data common in two populations as input, LD (D', or r^2, or signed r^2) between every pair of SNPs in a window is calculated. The window moves forward one SNP each time. In each window, a symmetric LD matrix for each population is calculated, and the difference of inter-population

LD difference is measured by raw score calculated using seven different methods. For genome-wide assessment, the raw score is standardised across the whole genome, and only the standardised scores that are larger or less than the predefined quantiles are defined as candidate regions of significant LD difference. The permutation test that randomly shuffles the label of populations is used to define significant LD difference regions.

Whole-exome sequencing of Alzheimer disease

A set of 246 APOE ε4 allele negative AD cases and 172 normal controls were enrolled in the study. Genomic DNA was isolated from the whole blood by using QIAamp DNA Blood Mini Kit (Qiagen, Hilden, Germany) in accordance with protocols. Coding regions were captured using the TruSeq Kit (Illumina, California, USA). The Illumina HiSeq 2000 (Illumina, California, USA) platform was used to generate 100 base-pair (bp) paired-end sequences, according to the manufacturer protocols.

Estimation of HLA types

First, sequence reads obtained by whole-exome sequencing were aligned to the genomic HLA sequences that were constructed from the international immunogenetics project HLA (IMGT/HLA) database using BWA-MEM. Then, the expected read counts on HLA class I (HLA-A, HLA-B, and HLA-C) and class II (HLA-DQA1, HLA-DQB1, and HLA-DRB1) alleles were estimated by variational Bayesian inference statistical framework in HLA-VBSeq.

HLA alleles association analysis

Pearson Chi-squared test or Fisher's exact test was performed on a 2×2 contingency table, which contains the counts of minor and major alleles for a single locus in cases and controls. Logistic and linear regression methods allow multiple covariates when testing for allele and amino acid association. The covariates can be either continuous or binary. A genotype is coded as 0, 1, or 2, depending on the number of effect allele it carries and which genetic model is tested.

We developed a Python package called PyHLA (https://github.com/felixfan/PyHLA) for HLA association analysis. PyHLA is a tailor-made, easy to use, and flexible tool designed specifically for the association analysis of the HLA types imputed from genome-wide genotyping and next-generation sequencing data. PyHLA provides functions for association analysis, zygosity tests, and interaction tests between HLA alleles and diseases. Monte Carlo permutation and several methods for multiple testing corrections were also implemented.

Results

A set of 246 APOE ε4 allele negative AD cases (70% female; 80.58±7.25 years old) and 172 normal controls (67% female; 78.5±6.27 years old) were analysed. HLA types were estimated from whole-exome sequencing data using HLA-VBSeq. HLA alleles association analysis was performed by using PyHLA.

Under allelic model, each allele was compared with the other alleles. HLA-DRB1*07:01 was inversely associated with AD (odds ratio=0.65, P=0.0027), whereas HLA-DQB1*03:01 was associated with AD (odds ratio=3.08, P=0.0017).

Under recessive model, individuals who carry two copy of the allele were compared to individuals who carry one or zero copy of the allele. HLA-C*03 was inversely associated with AD (odds ratio=0.29, P=0.0051), whereas HLA-DRB1*09:21 was strongly associated with AD (odds ratio=10.6, P=5.4e-7).

Under additive model, individuals who carry zero, one, and two copy of the allele were coded as 0, 1, and 2, respectively. Logistic regression was used to analyse the association. HLA-DRB1*07:01 was strongly inversely associated with AD (odds ratio=0.11, P=5.36e-7), whereas HLA-DRB1*09:21 was strongly associated with AD (odds ratio=10.6, P=1.02e-4).

The 1000 Genomes Project phase 3 data contains 2504 individuals from 26 populations. Overall, 33 722 SNPs within the HLA region with minor allele frequency >1% in all 26 populations were kept for analysis. We first examined LD difference across the HLA region between East Asian and European populations. Window size was set to 50 SNPs and r^2 was used to measure LD. We took the region with standardised score that was higher than the score at the 99th percentile or lower than the score at the 1st percentile as a candidate LD difference region. Only a small fraction of the candidate LD different regions was overlapped among different methods that measure LD difference between two populations. Most candidate LD different regions were unique to each method. The candidate LD different regions were consistent across different window sizes, although the smaller window size tended to identify higher resolution boundaries of the candidate regions.

About 50% to >90% of the candidate LD different regions were different between super population pairs, indicating strong evidence of inter super populations LD difference in MHC regions. The East Asian super population contained five populations. Even within the same super populations, the inter-population LD difference in MHC region still exists.

The tag SNP is a representative SNP in a high LD genome region. The pairwise tag SNP selection method in Tagger was used to select the tag SNPs by using the stand-alone programme Haploview,

which has implemented Tagger. LD r2 threshold of 0.8 was used for the selection of tag SNPs. Among the tag SNPs in the eleven populations, the Japanese population had the highest tagging efficiency (4.75), and the African ancestry population had the lowest tagging efficiency (Table). The results suggested that the tag SNPs are likely to differ between populations and the tagging efficiency are also different between different regions across the MHC regions (Fig 1). This may be one possible reason of failure replication of association in a different population.

Although haplotypes were mainly used as reference for imputation of unobserved genotypes in genome-wide association studies and phasing of other individuals. Haplotypes may enable susceptibility gene identification in complex diseases more effectively than individual SNPs because they can capture the LD patterns of a genomic region more completely. The results suggested that the length and frequency of the most common haplotype blocks vary greatly throughout the MHC region, as well as among different populations (Fig 2). The haplotype difference should be taken into consideration when planning to replicate haplotype-based association analysis.

Discussion

The current study investigated HLA alleles in southern Chinese patients with AD. The HLA typing association analysis suggested that HLA-DRB1*07:01 is significantly less prevalent in patients with AD, and that HLA-DQB1*03:01 is significantly more prevalent in patients with AD. The homozygous of HLA-C*03 is significantly less prevalent in patients with AD than controls, and homozygous of HLA-DRB1*09:21 is significantly more prevalent in patients with AD than controls.

TABLE. tag SNPs in the major histocompatibility complex of eleven populations

Populations	No. of samples	No. of SNPs	No. of tags	Ratio	No. of specific	No. of common
ASW	53	4480	1512	2.96	137	112
CEU	112	4405	1067	4.13	104	
CHB	137	4209	1181	3.56	92	
CHD	109	4013	1048	3.83	81	
GIH	101	4314	1248	3.46	126	
JPT	113	4069	856	4.75	80	
LWK	110	4471	1435	3.12	156	
MEX	58	4493	1326	3.39	120	
MKK	156	4506	1605	2.81	160	
TSI	102	4556	1361	3.35	111	
YRI	147	4341	1352	3.21	114	

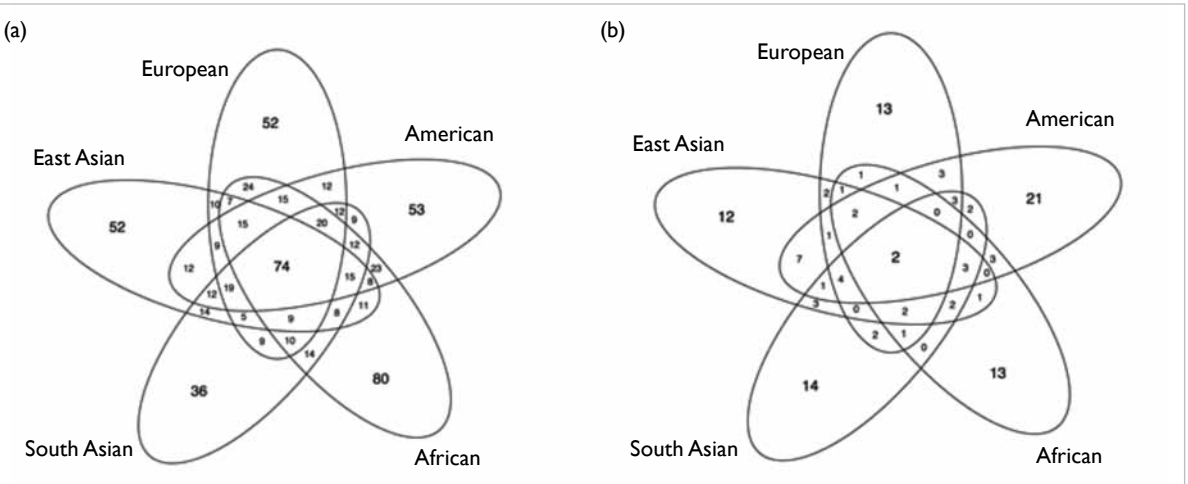

FIG 1. Number of shared tag SNPs (a) from rs1634794 to rs9265631 and (b) from rs805297 to rs805297 among different populations. In each region, 1000 SNPs with MAF of >0.05 were included. Pairwise tagging algorithm was used with r^2>0.8.

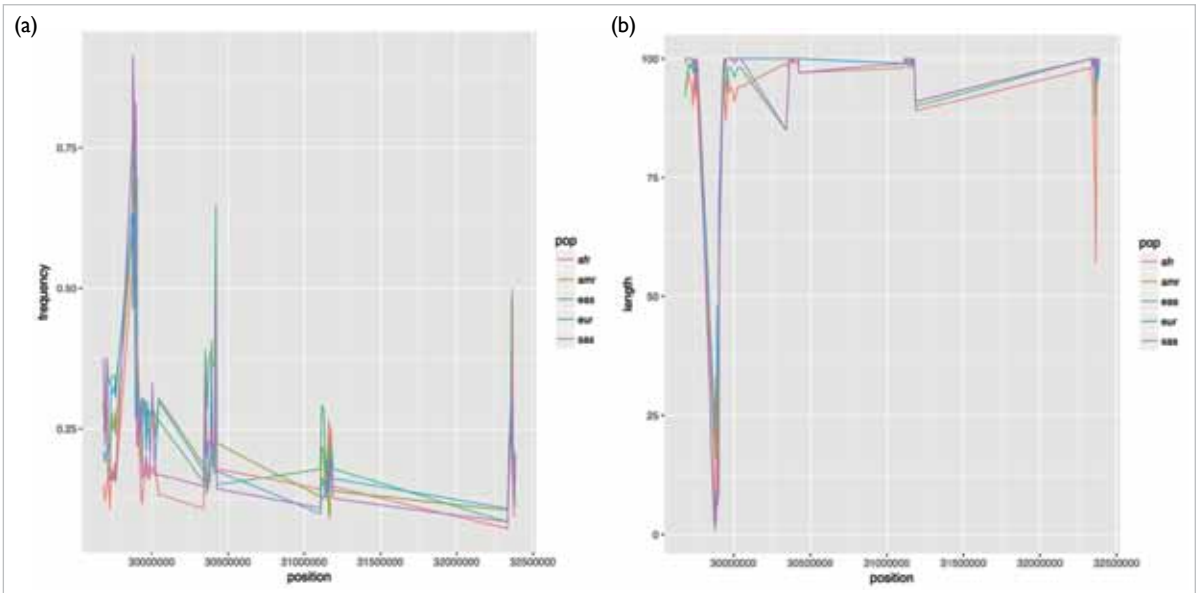

FIG 2. (a) Frequency and (b) length of the most common haplotype throughout the major histocompatibility complex region and across the populations

A meta-analysis of 74 046 individuals identified 11 new susceptibility loci for AD.[3] HLA-DRB5-DRB1 region is the most significant region. Association analysis of 48 clinically diagnosed elderly AD cases and 44 pathologically confirmed elderly controls showed an increased frequency of DRB1*03 and decreased frequency of DRB1*09 in the late-onset AD cases.[4] HLA-DRB1/DQB1 gene variants appeared to modulate the alteration of the left posterior cingulate volume, hence modulating the susceptibility of AD.[5]

In the current study, HLA-DRB1*09 was more prevalent in patients with AD, which is not consistent with previous study. This may be caused by the smaller sample size of previous study or the population structure. There is no previous study about association of HLA-C*03 and AD. The current study provides the first association study of higher resolution HLA alleles and AD in a bigger sample size.

The programme quantLD can handle larger data and is more efficient for imputation by using multithreading, compared with varLD. More methods to measure the LD difference are also available in quantLD. We compared LD difference between populations in 1000 genomes project data using quantLD. Results suggested that there are LD difference between populations. Knowledge of LD difference in a region is valuable when replicate association signals in this region across populations. For genotype imputation, the procedure for the region of LD difference may need to be different from the region with LD difference to produce confident genotypes.

Acknowledgements

This study was supported by the Health and Medical Research Fund, Food and Health Bureau, Hong Kong SAR Government (#01121726). We thank Dana Wong for technical support.

Results from this study have been published in: Li M, Li J, Li MJ, et al. Robust and rapid algorithms facilitate large-scale whole genome sequencing downstream analysis in an integrative framework. Nucleic Acids Res 2017;45:e75.

References

1. Complete sequence and gene map of a human major histocompatibility complex. The MHC sequencing consortium. Nature 1999;401:921-3.
2. Horton R, Wilming L, Rand V, et al: Gene map of the extended human MHC. Nat Rev Genet 2004;5:889-99.
3. Lambert JC, Ibrahim-Verbaas CA, Harold D, et al. Meta-analysis of 74,046 individuals identifies 11 new susceptibility loci for Alzheimer's disease. Nat Genet 2013;45:1452-8.
4. Neill D, Curran MD, Middleton D, et al. Risk for Alzheimer's disease in older late-onset cases is associated with HLA-DRB1*03. Neurosci Lett 1999;275:137-40.
5. Wang ZX, Wang HF, Tan L, et al. Effects of HLA-DRB1/DQB1 genetic variants on neuroimaging in healthy, mild cognitive impairment, and Alzheimer's disease cohorts. Mol Neurobiol 2017;54:3181-8.

Novel PCDH10-Wnt-MALAT1 regulatory axis in endometrioid endometrial adenocarcinoma

Y Zhao, Y Yang, J Trovik, K Sun, L Zhou, P Jiang, TS Lau, EA Hoivik, HB Salvesen, H Sun, H Wang *

KEY MESSAGES

1. Protocadherin 10 (PCDH10) is silenced in endometrioid endometrial cancer through promoter hypermethylation.
2. Ectopic expression of PCDH10 inhibits tumour growth and induces cell apoptosis.
3. Transcriptomic analysis revealed that PCDH10 expression down-regulates metastasis-associated lung adenocarcinoma transcript 1 (MALAT1). Further mechanistic studies uncovered that MALAT1 expression is transcriptionally induced by Wnt/β-catenin signalling.
4. We uncovered a novel PCDH10-Wnt/β-catenin-MALAT1 regulatory axis that contributes to development and progression of endometrioid endometrial cancer.

Hong Kong Med J 2019;25(Suppl 7):S17-22
HMRF project number: 01120446

[1] Y Zhao, [1] Y Yang, [2,3] J Trovik, [4] K Sun, [1] L Zhou, [4] P Jiang, [1] TS Lau, [2,3] EA Hoivik, [2,3] HB Salvesen, [4] H Sun, [1] H Wang

[1] *Department of Obstetrics and Gynaecology, The Chinese University of Hong Kong*
[2] *Department of Gynecology and Obstetrics, Haukeland University Hospital, Bergen, Norway*
[3] *Centre for Cancer Biomarkers, Department of Clinical Science, University of Bergen, Norway*
[4] *Department of Chemical Pathology, The Chinese University of Hong Kong*

* Principal applicant and corresponding author: huating.wang@cuhk.edu.hk

Introduction

Endometrioid endometrial cancer (EEC) accounts for 80% to 90% of all endometrial cancers. Its key mutational events have been characterised, but the underlying molecular mechanisms remain poorly elucidated. We discovered a novel mir-193-YY1-APC regulatory axis that exerts functional roles in EEC development.[1] In this study, we investigated the tumour suppressive function of protocadherin 10 (PCDH10) in EEC. PCDH10 was proposed as a tumour suppressor, and its inactivation secondary to promoter hypermethylation has been detected in multiple cancers. Restoration of PCDH10 could inhibit cell growth, reduce clonogenicity, restrain cell invasion, and induce cell apoptosis.[2] The link between PCDH10 and EEC is unknown, and the molecular mechanisms await exploration. LncRNAs are RNA species over 200 nucleotides in length and play an important role in transcriptional regulation. LncRNAs are deregulated in different cancer contexts, including metastasis-associated lung adenocarcinoma transcript 1 (MALAT1). Since its discovery as a prognostic factor for lung cancer metastasis, MALAT1 has been shown to be broadly up-regulated in a variety of cancer entities and to play critical roles in distinct cancer hallmark capabilities.[3] However, study of MALAT1 function in EEC is still lacking, and the transcriptional regulation of MALAT1 expression and the causes behind its deregulation are barely explored.

Methods

A total of 76 cases of primary EEC and 45 cases of normal tissues were used in this study. All specimens, clinical information, and procedures were approved by the Clinical Research Ethics Committee of The Chinese University of Hong Kong.

In a xenograft mouse model, 5×10^6 of control or PCDH10 stably expressing HEC-1-B cells were subcutaneously injected into the left and right flanks of the female athymic nude mice (n=5 for each group). All animal experiments were approved by Animal Experimentation Ethics Committee of The Chinese University of Hong Kong.

Human EEC cell lines were obtained from American Tissue and Cell Culture and cultured as recommended.

A 516 bp fragment harbouring TCF4 binding site was amplified from genomic DNA and cloned into pGL3-basic vector. The mutant reporter was generated by mutating the TCF4 binding motif from CTTTGAA to CTTTGCG.

An RNA antisense probe was in vitro transcribed corresponding to 6871-7224 bp of MALAT1 (RefSeq accession, NR_002819).

ChIP assays were carried out as described previously.[4] 5 μg of antibodies against β-catenin or equal amount isotype IgG was used for each 2×10^7 cell per ChIP. Immunoprecipitated genomic DNA was resuspended in 15 μL of water. PCR was then performed with 1 μL of DNA as a template on a 7900HT system.

The difference of PCDH10 mRNA expression between tumour and adjacent non-tumour tissues was analysed by the Mann-Whitney *U* test. For analysing the association of MALAT1 ISH scoring with clinical parameters, Pearson's Chi-square test was used. Statistical significance between two groups was assessed by Student's *t*-test. All tests were two sided, and a P value of <0.05 was considered statistically significant.

Results

PCDH10 is down-regulated in EEC through promoter hypermethylation

We examined PCDH10 mRNA expression in EEC cells lines and micro-dissected EEC tumour samples using normal endometrial tissue as controls. PCDH10 was significantly down-regulated in 76 tumour samples and all five cell lines, compared with 45 normal controls (Fig 1a). Aberrant hypermethylation in a CpG island (+8 ~ -328 bp upstream TSS) of PCDH10 promoter was detected in EEC tumours but not in normal endometrial tissues (Fig 1b). This finding was confirmed by analysing the genome-wide methylation data generated by The Cancer Genome Atlas project. Our analysis results from a cohort of 208 EEC patients and 34 normal controls showed a marked hypermethylation on the above region of PCDH10 promoter in EEC samples. Consistently, when treated with demethylation agent, 5-Aza, the promoter hypermethylation was markedly reduced and PCDH10 expression was restored (Fig 1c). Collectively, these results demonstrated that PCDH10 is down-regulated in EEC through its promoter hypermethylation.

PCDH10 restoration inhibits proliferation and induces apoptosis in EEC cells

We performed gain-of-function study by overexpressing PCDH10 in EEC cells. Successful restoration of PCDH10 was found to inhibit cell proliferation as revealed by cell counting and MTS assay (Fig 1d). Furthermore, overexpression of PCDH10 impeded their abilities to grow in an attachment-independent manner (Fig 1e). In addition, a marked increase in the number of subG1 cells was detected in both AN3CA and HEC-1-B cells (Fig 1f), suggesting that PCDH10 may lead to cell apoptosis. Consistently, the Annexin V-PI double staining and TUNEL assays revealed that the number of apoptotic cells was significantly increased upon PCDH10 overexpression. Collectively, these results concluded that PCDH10 is a pro-apoptotic factor in EEC cells.

RNA-sequencing reveals MALAT1 as a downstream factor of PCDH10

We performed a genome-wide analysis to globally characterise PCDH10-affected transcriptomic changes. Among all potential targets, MALAT1 is one of the most significant targets downregulated upon overexpression of PCDH10. MALAT1 is well known to have an oncogenic role and involved in diverse processes of cancer development including cell proliferation, apoptosis, migration, and metastasis; nevertheless, its role in EEC has not been investigated. MALAT1 is abundantly expressed in EEC cells thus making the functional study relatively easy and feasible in a short period of time. MALAT1 is well studied in many systems and necessary reagents are relatively easy to obtain

The RNA-seq data revealed that MALAT1 was decreased by approximately 70% in PCDH10 expressing cells (Fig 1g), which is further validated by independent qRT-PCR analyses (Fig 1h). To test whether MALAT1 is functionally downstream of PCDH10, we examined the effect of MALAT1 by using two siRNAs. Successful decrease of MALAT1 led to a significant delay in cell proliferation as revealed by cell counting assay and MTS assay (Fig 2a). Furthermore, siMALAT1 treatment induced a striking increase in apoptotic cell population (Fig 2b). Altogether the above findings suggested that MALAT1 knockdown phenocopied PCDH10 overexpression effect in EEC cells. Overexpression of MALAT1 reversed the inhibitory effect of PCDH10 on EEC cell growth (Fig 2c).

PCDH10 suppresses MALAT1 transcription through inhibiting WNT/β-catenin signalling

PCDH-gamma was found to negatively regulate Wnt/β-catenin signalling.[5] We speculated that loss of PCDH10 may induce MALAT1 expression through activation of Wnt signalling. We examined the effect of PCDH10 restoration on Wnt signalling. PCDH10 overexpression caused a sharp decrease of several Wnt targets, including LEF1, TCF1, and c-MYC (Fig 2d) as well as Wnt signalling reporter activity (Fig 2e). Stimulation of Wnt signalling by lithium chloride led to a mild but significant increase of MALAT1 expression (Fig 2f). Moreover, we analysed publicly available TCF4 ChIP-seq data generated from various cell lines. In all the five cell lines, two TCF4 binding peaks proximal to the TSS of MALAT1 were detected and a consensus binding motif of TCF4 was found in the promoter region (+78 to +88 bp) [Fig 2g]. We cloned this region into a luciferase reporter (wild type) and found its activity was induced upon lithium chloride treatment; however, the response was lost when the TCF binding site is mutated (Mut) [Fig 2h]. Furthermore, PCDH10 over-expression could suppress the wild type but not the Mut activities (Fig 2i), suggesting PCDH10 regulates MALAT1 transcription through inhibiting Wnt signalling. We performed ChIP

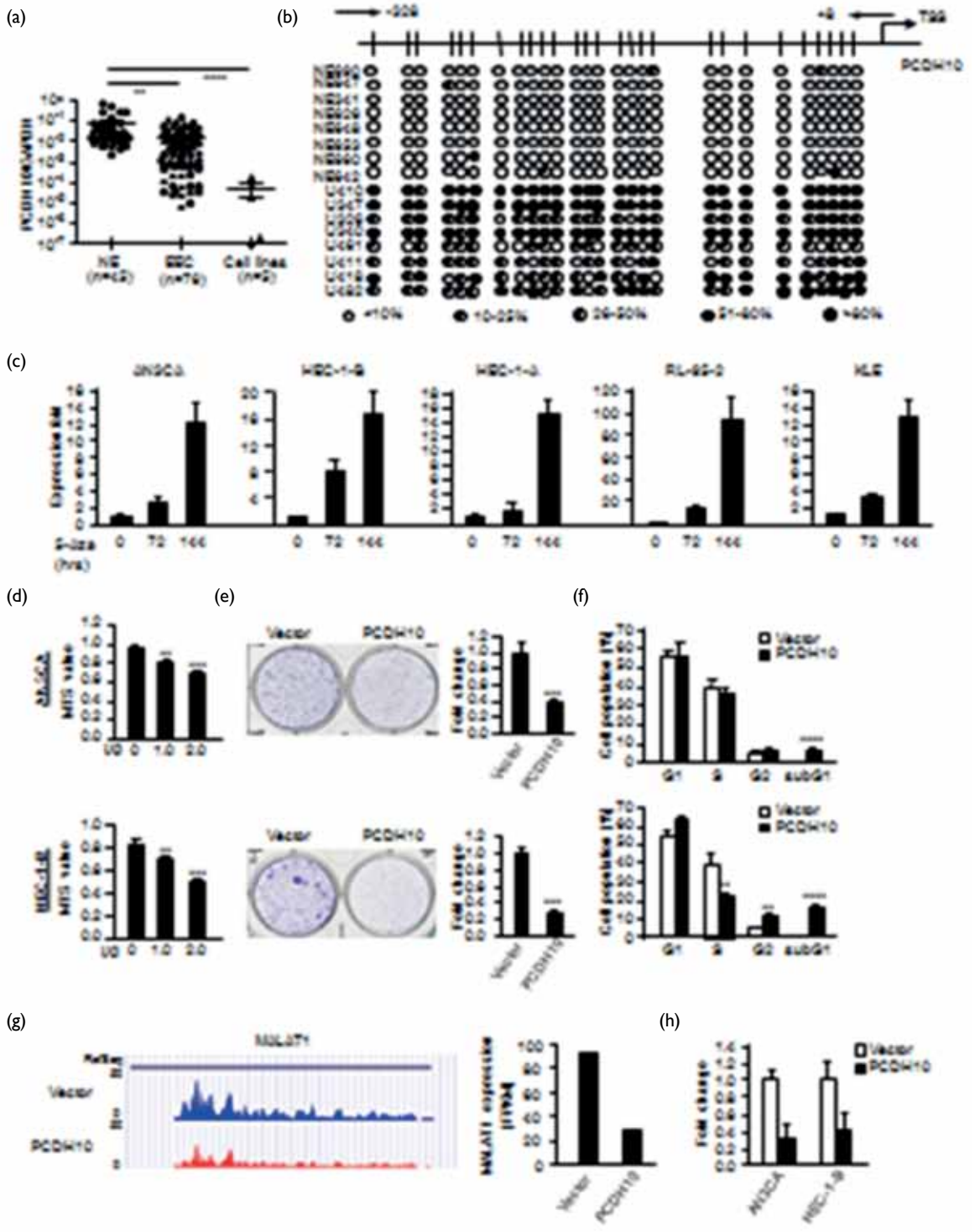

FIG 1. PCDH10 is down-regulated in endometrioid endometrial cancer (EEC) cells through promoter hypermethylation and functions to inhibit EEC cell proliferation and to induce cell apoptosis. (a) Expression of PCDH10 in microdissected normal endometrial tissues (NE, n=45), EEC primary tumours (EEC, n=76), and five EEC cell lines. (b) Methylation status of CpG sites in the PCDH10 promoter in 8 normal endometrial and 8 EEC samples assayed by bisulfate genomic sequencing. A 336-bp region (-328 ~ +8) spanning the core promoter harbouring 27 CpG sites was analysed. The degree of methylation was measured as percentage of methylated cytosines from seven randomly sequenced colonies. (c) Relative PCDH10 expression levels in five EEC cell lines treated with 5-Aza for the indicated times. (d) Cell proliferation in the above transfected cells was measured by MTS assay. (e) Monolayer colony formation assay was performed in the above control or PCDH10 expressing cells. The number of colonies was counted from three independent experiments. (f) Relative cell numbers in each cell cycle phase were determined by FACS of the PI-stained staining vector control or PCDH10 expressing cells. Percentages of cells in each phase (G1, S, G2, subG1) are represented. (g) Differential expression of MALAT1 transcripts determined by RNA-seq, shown as wiggle tracks on the UCSC genome browser. The expression values of MALAT1 in FPKM. (h) MALAT1 RNA expression was measured in AN3CA and HEC-1-B cells expressing vector or PCDH10 using qRT-PCR.

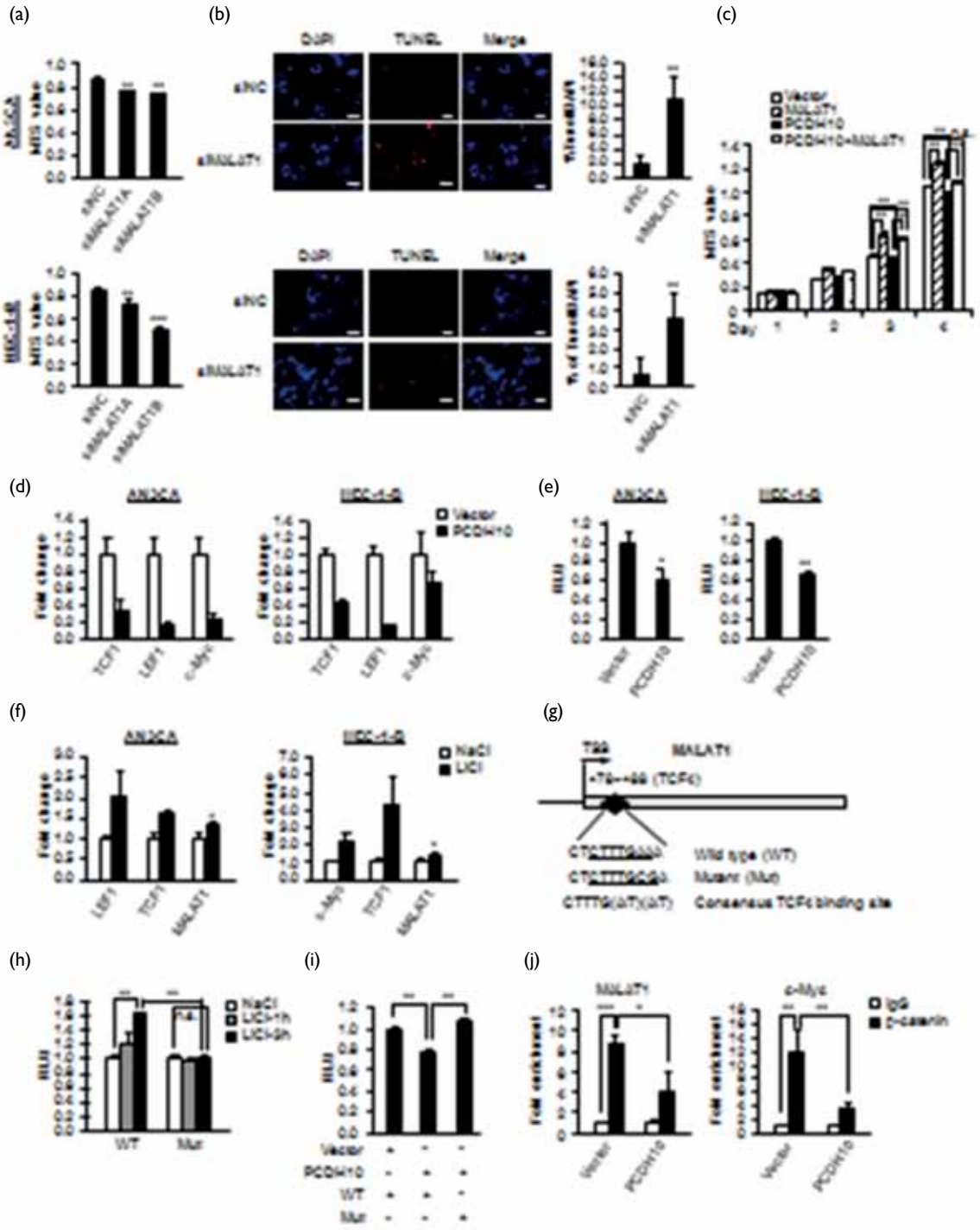

FIG 2. MALAT1 is a functional downstream of PCDH10 and PCDH10 inhibits MALAT1 transcription through Wnt/β-catenin signalling pathway. (a) Depletion of MALAT1 by siRNA oligos in AN3CA and HEC-1-B cells. Two siRNAs targeting MALAT1 (siMALAT1A and siMALAT1B) were used with a scramble sequence as control (siNC). Proliferation of the above transfected cells was determined by MTS assay. (b) Cell apoptosis was determined by TUNEL assay in AN3CA and HEC-1-B cells transfected with siMALAT1 or siNC. The index of TUNEL-positive cells is calculated. (c) HEC-1-B cells stably expressing PCDH10 or control vector were transiently transfected with MALAT1 expressing or a vector control plasmid, respectively. Cell proliferation was measured using MTS value at the indicated days after seeding. (d) PCDH10 decreases the mRNA expression levels of c-Myc, LEF1 and TCF1, in both AN3CA and HEC-1-B cells. (e) Transient expression of PCDH10 inhibits TOP-flash luciferase reporter activity in the above cells. (f) Expression of MALAT1 was increased by lithium chloride treatment; c-Myc, LEF1 or TCF1 expression was used as positive controls. (g) Schematic illustration of the promoter region of MALAT1 gene. The predicted TCF4 binding site with genomic location (+78 ~ +88) was displayed; wild type, mutant, and the consensus TCF binding sequences were indicated below. (h) Lithium chloride treatment increased the activity of the wild type but not the Mut reporter. (i) PCDH10 inhibits the wild type but not the Mut reporter. Values were normalised by renilla levels. (j) ChIP-PCR detection of the β-catenin enrichment on the TCF binding site in HEC-1-B cells stably expressing PCDH10 or vector control. c-Myc genomic region harbouring a TCF binding site was used as a positive control. Enrichment values are relative to input.

to detect β-catenin enrichment on MALAT1 promoter. Expectedly, a robust enrichment of β-catenin was found on the identified TCF4 site and the enrichment was significantly diminished upon PCDH10 overexpression (Fig 2j). Together, these data demonstrated that PCDH10 suppresses MALAT1 expression through impairing β-catenin binding to its promoter.

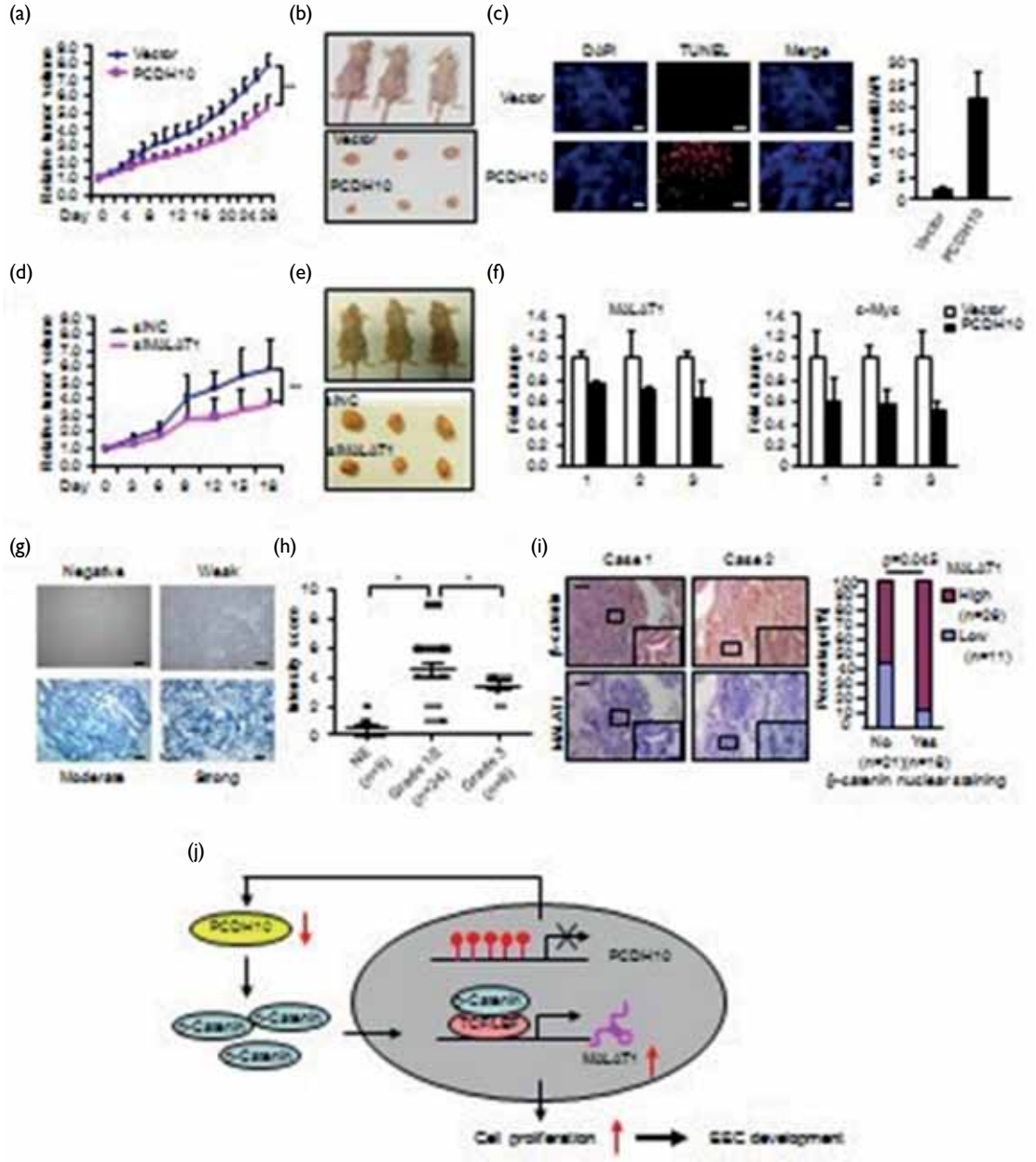

FIG 3. ***PCDH10*-MALAT1 regulatory axis *in vivo*.** (a) *PCDH10* attenuates subcutaneous tumour growth in a mouse xenograft model. Relative tumour volumes are shown with respect to day 0 where the volumes were set to 1. (b) Mice were sacrificed at the end of the treatment and images were taken along with the dissected tumours from three representative mice. (c) *In situ* cell apoptosis in xenograft tumours was determined by TUNEL staining of the tumour sections. (d) Knockdown of MALAT1 by intratumoural injection of siRNA oligos inhibits subcutaneous tumour growth in a mouse xenograft model. (e) Images of mice and the dissected tumours were taken at the end of the treatment. (f) The expression of MALAT1 and c-Myc was decreased in *PCDH10* xenograft tumours. (g) In situ hybridisation (ISH) detection of MALAT1 RNA in normal endometrial tissues and endometrioid endometrial cancer (EEC) patient samples. Representative images with various levels of staining (negative from normal tissue, weak, moderate or strong from tumour tissues). (h) The association of the ISH staining scores with grades of tumour (1/2 or 3). (i) IHC staining of β-catenin and ISH staining of MALAT1 on sequential sections of 37 EEC specimens. Representative β-catenin and MALAT1 staining images are shown in three EEC cases MALAT1 and nuclear β-catenin staining levels above were scored and the anti-correlation between MALAT1 ISH score and nuclear β-catenin IHC score in 37 EEC samples was shown. (j) A model of PCDH10-Wnt/β-catenin-MALAT1 axis in EEC development. In EEC tumours, the promoter region of *PCDH10* is highly methylated, resulting in the down-regulation of *PCDH10*, which subsequently induces the expression of MALAT1 through activating Wnt/β-catenin signalling. The expression of MALAT1 leads to increased cell proliferation which contributes to EEC development.

PCDH10-MALAT1 regulatory axis in vivo

We evaluated the function of PCDH10-MALAT1 regulatory axis in vivo. We found PCDH10 overexpression markedly delayed tumour growth (n=5, P<0.01, Fig 3a, b) and caused a severe cell apoptosis in vivo (Fig 3c), which was in agreement with its pro-apoptotic effect. To illustrate the effect of MALAT1, siRNA oligos were injected into the HEC-1-B xenograft tumour. A comparable phenotype as PCDH10 over-expression could be observed in siMALAT1 group (Fig 3d, e). We also detected reduced level of both MALAT1 and c-Myc in PCDH10 overexpressing tumours (Fig 3f), suggesting the existence of PCDH10-Wnt-MALAT1 axis in the xenografts.

To validated the above findings in EEC clinical samples, we examined the MALAT1 expression by in situ hybridisation on the paraffin sections. A much higher level was found in EEC samples as compared with normal tissues (Fig 3g). In addition, a strong MALAT1 signalling appeared to be associated with low histologic grade (grade 1/2 versus 3) [P=0.028, Fig 3h].

Analyses of tissue microarray data revealed that high expression of MALAT1 was linked with hyperplasia (P=0.017), menopausal status (P=0.028), no recurrence (P=0.032), and low metastasis potential (P=0.041). Further exploring The Cancer Genome Atlas data from a large cohort of EEC samples (n=253), we detected a reverse association between PCDH10 and MALAT1 (P=0.0324). Additionally, the expression level of MALAT1 by ISH staining is found strongly correlated with the total or nuclear level of β-catenin by IHC staining (Fig 3i). Altogether, these analyses confirmed the presence of PCDH10-Wnt/β-catenin-MALAT1 regulation in clinical samples.

Discussion

We identified PCDH10 as a tumour suppressor in EEC. Our results showed that PCDH10 promoter is hypermethylated through analysis of locally collected EC samples and analysing The Cancer Genome Atlas data from worldwide EEC samples. Functional studies revealed that restoration of PCDH10 successfully reduced cell growth and induced cell apoptosis, in keeping with what was uncovered in other cancers. Notably, we could not recapitulate all functional features of PCDH10 demonstrated in other studies and the impact of PCDH10 on cell cycle also differs between two EEC cell lines, which may reflect cell type and cancer type specific roles of PCDH10.

Our findings uncovered the transcriptomic influence exerted by PCDH10. Moreover, we identified MALAT1 as a functional downstream target of PCDH10 and showed that MALAT1 plays an oncogenic role in EEC. We demonstrated that MALAT1 is positively associated with hyperplasia, and negatively with metastasis, suggesting its predictive value as a molecular biomarker. The positive correlation of MALAT1 with hyperplasia and low grade EEC implies that dysregulation of MALAT1 is an early event in EEC development.

We provide novel insights into how PCDH10 acts on MALAT1 through modulating Wnt/β-catenin signalling. We identified MALAT1 as a direct transcriptional target of Wnt/β-catenin in EEC cells. According to ChIP-seq data from ENCODE, the TCF binding on this site is present in multiple cancer cell lines, thus Wnt regulation of MALAT1 likely occurs as a general pathway in various cancers.

Collectively, we identified a novel regulatory axis, PCDH10-Wnt-MALAT1 in the effort of elucidating the tumour suppressive function of PCDH10 (Fig 3j) and showed PCDH10 and lncRNA function in EEC and elucidated the transcriptional regulation of MALAT1.

Acknowledgements

This study was supported by the Health and Medical Research Fund, Food and Health Bureau, Hong Kong SAR (#01120446) and a GRF grant to HW (2041474) from the Research Grants Council and funding from the Department of Obstetrics and Gynaecology, The Chinese University of Hong Kong.

References

1. Ying J, Li H, Seng TJ, et al. Functional epigenetics identifies a protocadherin PCDH10 as a candidate tumor suppressor for nasopharyngeal, esophageal and multiple other carcinomas with frequent methylation. Oncogene 2006;25:1070-80.
2. Gutschner T, Hammerle M, Diederichs S. MALAT1: a paradigm for long noncoding RNA function in cancer. J Mol Med (Berl) 2013;91:791-801.
3. Lu L, Sun K, Chen X, et al. Genome-wide survey by ChIP-seq reveals YY1 regulation of lincRNAs in skeletal myogenesis. EMBO J 2013;32:2575-88.
4. Dallosso AR, Hancock AL, Szemes M, et al. Frequent long-range epigenetic silencing of protocadherin gene clusters on chromosome 5q31 in Wilms' tumor. PLoS Genet 2009;5:e1000745.

Influenza virus infections in Hong Kong in 2013-14: a community-based longitudinal seroepidemiological study

BJ Cowling *, JSM Peiris, KO Kwok

KEY MESSAGES

1. We conducted a longitudinal serologic study and estimated that between 3% to 7% of unvaccinated people in Hong Kong were infected in each of four influenza epidemics in 2013 and 2014.
2. Incidence of influenza virus infections was relatively low in children, in contrast to the very high incidence of infections reported in the 2009 pandemic.

Hong Kong Med J 2019;25(Suppl 7):S23-6
HMRF project number: 13120732

BJ Cowling, JSM Peiris, KO Kwok

School of Public Health, Li Ka Shing Faculty of Medicine, The University of Hong Kong

* Principal applicant and corresponding author: bcowling@hku.hk

Introduction

Influenza viruses are responsible for a considerable disease burden every year including hundreds of excess deaths and thousands of excess hospitalisations in Hong Kong.[1,2] When considering the impact of influenza epidemics, it is important to distinguish the incidence of infections from the severity of infections. In typical influenza epidemics, the highest incidence of infection usually occurs in school-age children,[3] whereas the severity of infections generally increases with age, with elderly people having a higher risk of death than adults or children.[4]

Many population-based serologic studies have been conducted during influenza pandemics to infer the cumulative incidence of infection with the new strain, which is referred to as the attack rate.[5,6] We conducted a longitudinal serologic study in Hong Kong in 2009-10 and estimated that in the first wave of the H1N1pdm09 pandemic the cumulative incidence of infection was 39% (31%-49%) for persons 3-19 years, 8.9% (5.3%-14.7%) for persons 20-39 years, 5.3% (3.5%-8.0%) for persons 40-59 years, and 0.77% (0.18%-4.2%) for persons 60 years or older.[7]

However, few serologic studies have been conducted for interpandemic influenza.[8] A community-based study in the United Kingdom included an average of 1000 persons in follow-up for 5 consecutive years, with a smaller number of participants in the initial years and a large number during 2009-10.[9] An average of 18% of people were infected with influenza each winter in the United Kingdom, with a particularly high incidence of H1N1pdm09 in children during 2009-10.[9]

The current study aimed to: (1) estimate the age-specific attack rate of influenza A and B in a representative group of households using three sets of paired serology between November 2012 and February 2015, and (2) evaluate the risk factors for influenza virus infection including age and vaccination status.

Methods

We previously had conducted a longitudinal study in the general community by collecting sera at regular intervals to investigate serologic evidence of influenza virus infection and estimated the cumulative incidence of infections across epidemics and across years.[10] The current study was a 2-year extension of that longitudinal study, covering periods of influenza activity in 2013 and 2014.

The longitudinal study was initiated in July 2009 in the early stages of the first wave of pandemic influenza A(H1N1)pdm09. We recruited participants from the general population across Hong Kong via random-digit dialling and from a subset of respondents in an earlier telephone survey that was also conducted with random-digit dialling.[7] In November 2009, a second study round was conducted by inviting all individuals who joined the previous round to take part again. Individuals who did not join the first round but were living with a round 1 participant were also eligible to join. These two study rounds constitute the first phase of this study (rounds 1-2). The second phase of this study involved three subsequent study rounds with the same design (rounds 3-5). The third phase of the study was the basis of the present project and began on 6 December 2013. All participants in the existing cohort were invited to continue. The target sample size was maintained by replacing dropouts with new participants using the same recruitment approach (ie, telephone survey sampling).

All participants who provided serum samples must be ≥2 years old and Hong Kong residents who reside in Hong Kong for ≥5 days a week. All household contacts of the participants must reside with the participants for ≥5 days a week in the same household. Priority was given to households with members participating in previous rounds. Participants were invited to visit the study clinic in Kowloon to provide blood samples. The rationale for the study was explained and written informed consent obtained. For children aged 8 to 17 years, written consent was obtained from both the child and their parent or guardian. For children aged 2 to 7 years, written consent was obtained from the parent or guardian. A blood sample of 4 mL was collected in a clotted blood tube, and basic demographics and relevant medical history including vaccination history were recorded on a standardised form.

TABLE 1. Baseline characteristics of participants in 2012-2014*

	2011 census	Round 5 (November 2012 to March 2013) [n=920]	Round 6 (December 2013 to March 2014) [n=846]	Round 7 (from October 2014 to January 2015) [n=855]
Number of households	-	613	576	611
Mean household size	2.88	3.08	2.86	2.83
Age, y				
0-9	7.2	8 (0.9)	10 (1.2)	3 (0.4)
10-19	11.1	43 (4.7)	44 (5.2)	46 (5.4)
20-39	13.2	82 (8.9)	69 (8.2)	83 (9.7)
30-39	14.7	62 (6.7)	62 (7.3)	56 (6.5)
40-49	17.3	163 (17.7)	130 (15.4)	113 (13.2)
50-59	16.7	277 (30.1)	248 (29.3)	246 (28.8)
60-69	9.4	192 (20.9)	179 (21.2)	198 (23.2)
≥70	10.4	90 (9.8)	99 (11.7)	109 (12.7)
Missing	0.0	3 (0.3)	5 (0.6)	1 (0.1)
Sex				
Female	51.6	553 (60.1)	507 (59.9)	345 (40.4)
Male	48.4	367 (39.9)	335 (39.6)	509 (59.5)
Missing	0.0	0 (0.0)	4 (0.5)	1 (0.1)
Occupation†				
Category 1	-	189 (20.5)	126 (14.9)	155 (18.1)
Category 2	-	217 (23.6)	222 (26.2)	235 (27.5)
Category 3	-	410 (44.6)	391 (46.2)	386 (45.1)
Category 4	-	97 (10.5)	79 (9.3)	76 (8.9)
Missing	-	7 (0.8)	28 (3.3)	3 (0.4)
Chronic disease				
Yes	-	422 (45.9)	387 (45.7)	363 (42.5)
No	-	488 (53.0)	455 (53.8)	492 (57.5)
Missing	-	10 (1.1)	4 (0.5)	0 (0.0)
Ever smoke				
Yes	-	141 (15.3)	79 (9.3)	91 (10.6)
No	-	763 (82.9)	759 (89.7)	764 (89.4)
Missing	-	16 (1.7)	8 (0.9)	0 (0.0)
Receipt of vaccination in prior session				
Yes	-	152 (16.5)	179 (21.2)	183 (21.4)
No	-	748 (81.3)	648 (76.6)	600 (70.2)
Missing	-	20 (2.2)	19 (2.2)	172 (8.4)

* Data are presented as % or No. (%) of participants unless otherwise stated

† Category 1 denotes managers and administrators, professionals and associate professionals; Category 2 clerks, service workers and shop sales workers, craft and related workers, plant and machine operators and assemblers, elementary occupations; skilled agricultural and fishery workers; and occupations not classifiable; Category 3, housekeepers, retired, economically inactive, and maid; Category 4, students

The haemagglutination inhibition assay was used to identify titre level of influenza strains in the serum samples. A/California/7/2009 (H1N1) and B/Brisbane/60/2007 (B/Victoria lineage) were tested antigens in rounds 5-7. Round 5 specimens were additionally tested for A/Perth/16/2009 (H3N2) and specimens from rounds 1-5 were additionally tested for A/Victoria/361/2011 (H3N2).

An infection was defined as a four-fold rise in antibody titres measured by the haemagglutination inhibition assay between consecutive serum samples. We estimated the cumulative incidence of infections indicated by serology in defined epidemics of particular influenza types/subtypes in 2013 and 2014. Cumulative incidence was estimated for four age-groups, and age-standardised estimates were made using the population distribution in the 2011 census. Logistic regression models were used to estimate odds ratio of new influenza virus infections versus different baseline characteristics.

Results

Of 920 participants in round 5, 629 (68%) extended the follow-up period to round 6 (from December 2013 to March 2014). In addition, 131 brand-new individuals and 86 participants from previous rounds other than round 5 were recruited in round 6, with a total of 846 participants. In round 7 from October 2014 to January 2015, 855 participants (587 from round 6, 191 new top-ups, and 77 old top-ups) were recruited. For rounds 5-7, we obtained 2621 serum samples from 1355 individuals.

Compared with the 2011 census, our study cohort over-sampled older adults (aged ≥50 years) and under-sampled younger individuals. Participants had similar baseline characteristics. The self-reported vaccination coverage ranged from 16% to 21% across three study rounds, and middle-aged adults or older adults reported vaccination most commonly (Table 1).

Of 12 distinct influenza epidemics identified from 2009 to 2014, five (epidemic number 8-12) were captured by our study period: the A(H3N2) epidemic in July to October 2013, the A(H3N2) epidemic in

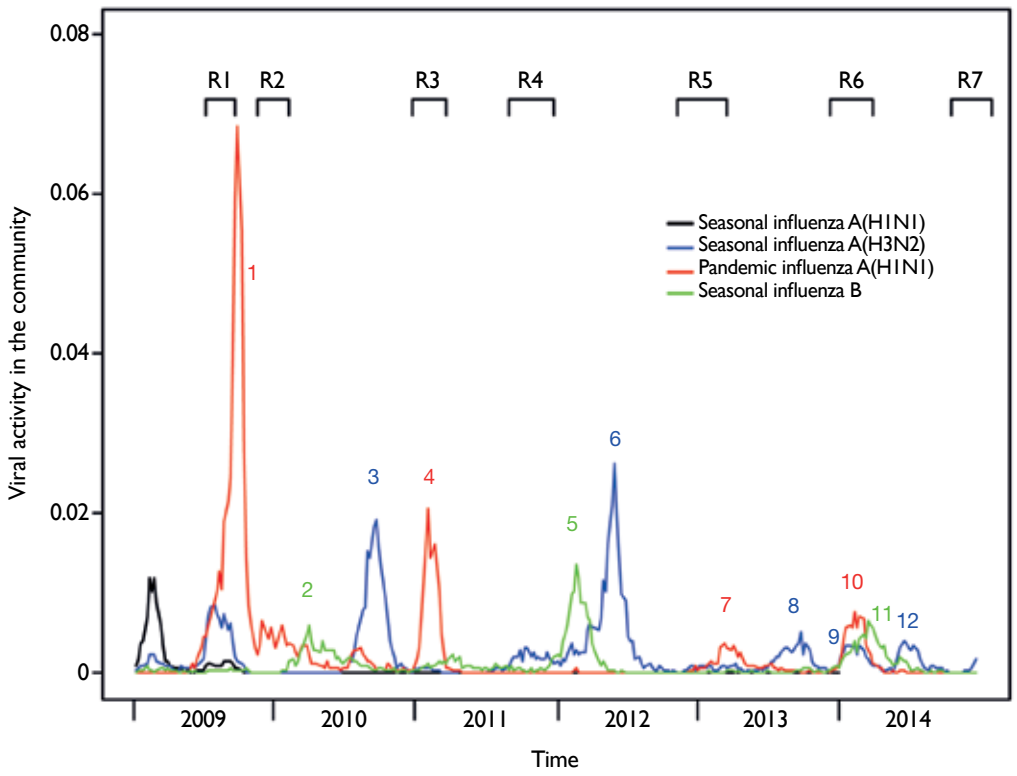

FIG. Study timeline and the community virus activity from 2009 to 2016

TABLE 2. Incidence of influenza virus infections confirmed by serology in different epidemics. The main circulating virus in each epidemic is highlighted in bold. Preference is given to subsequent study rounds that (almost) neatly bracket the epidemics. Study round selection is only eligible to epidemics of unique subtype between two subsequent study rounds.

Epidemic No.	Epidemic	Study rounds involved	Incidence (95% confidence interval) of influenza virus infection confirmed by serology		
			A/California/7/2009	A/Victoria/361/2011	B/Brisbane/60/2007
8	A(H3N2)	5,6	0.14 (0.12-0.17)	**0.11 (0.08-0.13)**	0.01 (0.01-0.02)
9	A(H3N2)*	-	-	-	-
10	H1N1pdm09	5,7	**0.10 (0.07-0.13)**	0.08 (0.06-0.11)	0.04 (0.02-0.06)
11	B	5,7	0.10 (0.07-0.13)	0.08 (0.06-0.11)	**0.04 (0.02-0.06)**
12	A(H3N2)	6,7	0.05 (0.04-0.07)	0.05 (0.04-0.07)	0.04 (0.02-0.05)

* This epidemic was bracketed by study rounds that were also surrounded by epidemics of the same subtype (ie, epidemic number 8 and 12).

TABLE 3. Age-specific and age-standard incidence estimates for the main circulating virus strain in each epidemic

	Incidence (95% confidence interval)			
	A/Victoria/361/2011 for epidemic 8	A/California/7/2009 for epidemic 10	B/Brisbane/60/2007 for epidemic 11	A/Victoria/361/2011 for epidemic 12
Age-group, y				
0-19	0.03 (-0.03 to 0.09)	0.00 (0.00 to 0.00)	0.04 (-0.04 to 0.12)	0.16 (0.03 to 0.29)
20-39	0.05 (0.00 to 0.10)	0.07 (0.00 to 0.13)	0.05 (-0.01 to 0.11)	0.06 (0.00 to 0.11)
40-59	0.05 (0.02 to 0.08)	0.05 (0.02 to 0.07)	0.01 (0.00 to 0.02)	0.03 (0.01 to 0.05)
≥60	0.05 (0.01 to 0.09)	0.06 (0.01 to 0.11)	0.05 (0.00 to 0.10)	0.05 (0.01 to 0.09)
Age-standardised to the 2011 population of Hong Kong	0.05	0.05	0.03	0.07

December 2013 to March 2014, the H1N1pdm09 epidemic in January to March 2014, the B epidemic in January to May 2014, and the A(H3N2) epidemic in June to July 2014 (Fig).

Proxied by the proportion of four-fold seroconversion to A/Victoria/361/2011, the new incidence attributable to the epidemic number 8 was 0.11 (95% confidence interval [CI]=0.08–0.13), whereas that to epidemic number 12 was 0.05 (95% CI=0.04-0.07) [Table 2]. The incidence of epidemic number 9 was not estimated because it was bracketed by study rounds that were also surrounded by epidemics of the same subtype. Age-specific and age-standard incidence estimates among unvaccinated individuals were calculated for the main circulating virus in each epidemic (Table 3). The incidence of new cases among older adults (aged ≥60 years) were similar across different epidemics (0.05-0.06). On the contrary, the incidence of new cases among young age groups (aged ≤19 years) was much more for epidemic number 12 (0.16) than other epidemics. Age and presence of chronic diseases were significant risk factors, whereas baseline H1N1 titre was significantly protective against subsequent H1N1 infection.

Discussion

Five epidemics were identified from 2013 to 2014. In our cohort, the overall incidence of infections was about 5% to 11% for influenza A epidemics and about 4% for influenza B epidemics during 2013-2014. Incidence was relatively low in children, in contrast to the very high incidence of infections reported in the 2009 pandemic.[7,11]

Age and chronic diseases were significantly associated with the risk of infection. Pre-existing baseline antibody titres were protective for A(H1N1), which has remained antigenically similar for a number of years, but not for A(H3N2) which has experienced much more antigenic drift.

This study has some limitations. The rounds of sera collection did not neatly bracket each epidemic, and we were unable to estimate the incidence of epidemic number 9. Models that account for individual titre boosting and waning to address non-bracketing issue are in development.[12] The four-fold rise in antibody titres across a prolonged period as an indicator of an influenza virus infection does not have perfect sensitivity and specificity for a true infection event because of waning in titres over time, temporal fluctuations in antibody titre for reasons not related to infection events, and the limitations in haemagglutination inhibition assays. In addition, we did not account for clustering in the analysis, which would have slightly widened the confidence intervals.

Acknowledgement

This study was supported by the Health and Medical Research Fund, Food and Health Bureau, Hong Kong SAR Government (#13120732).

References

1. Wu P, Goldstein E, Ho LM, et al. Excess mortality associated with influenza A and B virus in Hong Kong, 1998-2009. J Infect Dis 2012;206:1862-71.
2. Li CK, Choi BC, Wong TW. Influenza-related deaths and hospitalizations in Hong Kong: a subtropical area. Public Health 2006;120:517-24.
3. Wu JT, Cowling BJ, Lau EH, et al. School closure and mitigation of pandemic (H1N1) 2009, Hong Kong. Emerg Infect Dis 2010;16:538-41.
4. Wu JT, Ma ES, Lee CK, et al. The infection attack rate and severity of 2009 pandemic H1N1 influenza in Hong Kong. Clin Infect Dis 2010;51:1184-91.
5. Kelly H, Peck HA, Laurie KL, Wu P, Nishiura H, Cowling BJ. The age-specific cumulative incidence of infection with pandemic influenza H1N1 2009 was similar in various countries prior to vaccination. PLoS One 2011;6:e21828.
6. Van Kerkhove MD, Hirve S, Koukounari A, Mounts AW; H1N1pdm serology working group. Estimating age-specific cumulative incidence for the 2009 influenza pandemic: a meta-analysis of A(H1N1)pdm09 serological studies from 19 countries. Influenza Other Respir Viruses 2013;7:872-86.
7. Riley S, Kwok KO, Wu KM, et al. Epidemiological characteristics of 2009 (H1N1) pandemic influenza based on paired sera from a longitudinal community cohort study. PLoS Med 2011;8:e1000442.
8. Monto AS. Studies of the community and family: acute respiratory illness and infection. Epidemiol Rev 1994;16:351-73.
9. Hayward AC, Fragaszy EB, Bermingham A, et al. Comparative community burden and severity of seasonal and pandemic influenza: results of the Flu Watch cohort study. Lancet Respir Med 2014;2:445-54.
10. Horby PW, Laurie KL, Cowling BJ, et al. CONSISE statement on the reporting of Seroepidemiologic Studies for influenza (ROSES-I statement): an extension of the STROBE statement. Influenza Other Respir Viruses 2017;11:2-14.
11. Wu JT, Ho A, Ma ES, et al. Estimating infection attack rates and severity in real time during an influenza pandemic: analysis of serial cross-sectional serologic surveillance data. PLoS Med 2011;8:e1001103.
12. Tsang TK, Fang VJ, Perera RA, et al. Interpreting seroepidemiologic studies of influenza in a context of nonbracketing sera. Epidemiology 2016;27:152-8.

Innate immune defect predisposing to severe influenza in a Chinese population

KKW To *, J Zhou, YQ Song, IFN Hung, KY Yuen

KEY MESSAGES

1. Genetic polymorphisms in SFTPB and PDE3A genes are independently associated with severe A(H1N1)pdm09 infection.
2. Surfactant protein B has antiviral activity against influenza A(H1N1)pdm09 infection.
3. PDE3A is an antiviral host factor

Hong Kong Med J 2019;25(Suppl 7):S27-9
HMRF project number: 13120842

[1] KKW To, [1] J Zhou, [2] YQ Song, [3] IFN Hung, [1] KY Yuen

The University of Hong Kong:
[1] *Department of Microbiology*
[2] *School of Biomedical Sciences*
[3] *Department of Medicine*

* Principal applicant and corresponding author: kelvinto@hku.hk

Introduction

Influenza virus is a common cause of severe respiratory tract infection. However, most patients with influenza virus infection have only mild respiratory illness. Clinical risk factors for severe influenza include extremes of age, chronic medical illness, pregnancy, and obesity. Patients with severe influenza have been reported to have host genetic defects.[1]

Results from in vitro and animal studies may not be applicable to humans; most genes identified have not been validated in human studies. Moreover, most human studies have comprised mainly Caucasians; the allele frequency differs between ethnic groups, and results from other ethnic groups may not be applicable to the Chinese population. Most human studies did not take into account the differences in comorbidities between patients with severe and mild disease.

This study aimed to use genome-wide association study to identify innate immune defects that predispose Chinese patients to severe influenza virus infection.

Methods

We compared single nucleotide polymorphisms (SNPs) between 42 patients with severe influenza A(H1N1)pdm09 virus infection and 42 patients with mild infection using Genome-Wide Human SNP Array 6.0 (Affymetrix). Both groups were matched for age, sex, and number of risk factors. SNPs were identified for confirmation in another cohort of patients with influenza virus infection using MassARRAY System (Sequenom). Multivariate analysis was performed to control for confounding factors. In vitro studies were performed to confirm the antiviral effects of these genes.

Results

From the genome-wide association study, 30 SNPs were selected for analysis in the second cohort of patients (Table 1), in which the surfactant protein B gene (*SFTPB*) SNP rs1130866 was also significantly associated with severe disease in univariate analysis (odds ratio [OR]=1.928, 95% confidence interval [CI]=1.152-3.227, P=0.012) and multivariate analysis (OR=2.087, 95% CI=1.107-3.934, P=0.023). We then compared the frequency of rs1130866 alleles in patients and in general Han Chinese population (using data from the 1000 Genomes Project). The C allele was significantly associated with severe A(H1N1)pdm09 infection for both recessive pattern (OR=3.232, 95% CI=2.033-5.139, $P=5.6 \times 10^{-7}$) and dominant pattern of inheritance (OR=6.223, 95% CI=1.401-27.640, P=0.006) [Table 2]. We then tested the antiviral activity of surfactant protein B against influenza viruses, as *SFTPB* encodes for surfactant protein B. Plaque reduction assay showed that the IC_{50} of surfactant protein B were 8-24 nM for A(H1N1) and A(H7N9), but the IC^{50} for A(H3N2) and A(H5N1) were >125 nM.

In addition, the phosphodiesterase 3A gene (*PDE3A*) SNPs rs7314545 and rs6487132 were also over-represented (but not significantly [P=0.07]) in severe disease cases of the second cohort of patients. As the level of PDE3A has been shown to be downregulated in the heart of patients with dilated cardiomyopathy or ischaemic heart disease,[2] we re-analysed our second-cohort patients after exclusion of those with heart disease. In this group of patients without heart disease, rs7314545-CT or rs7314545-TT was over-represented in patients with severe disease than in patients with mild disease (17.0% [15/88] vs 8.1% [14/173], P=0.030; OR=2.334, 95% CI=1.071-5.087). Multivariate analysis showed that rs7314545-CT or rs7314545-

TABLE 1 Allelic P values between patients with severe and mild A(H1N1)pdm09 infection

Gene	Single nucleotide polymorphism	Allelic P value
ADIPOR2	rs1044471	>0.05
ADIPOR2	rs11612383	>0.05
ADIPOR2	rs4766415	>0.05
ADIPOR2	rs9300298	>0.05
C4BPA	rs9943077	>0.05
C7	rs3792648	>0.05
C7	rs7713409	>0.05
CARD8	rs2043211	>0.05
CXCL12	rs1801157	>0.05
DSCAM	rs2837657	>0.05
EPHB2	rs4655117	>0.05
HIVEP1	rs2228211	>0.05
HNF4G	rs1805099	>0.05
JAK2	rs10974944	>0.05
KLRK1/ NKG2D	rs4764430	>0.05
MAGI2	rs10279983	>0.05
MAGI3	rs1217228	>0.05
NCAM2	rs2226665	>0.05
NFKBIA	rs3138053	>0.05
PDE3A	rs6487131	>0.05
PDE3A	rs6487132	0.06839
PDE3A	rs7314545	0.06798
PDE4B	rs12029272	>0.05
RNASEL	rs11807829	>0.05
RNASEL	rs11807829	>0.05
SELP	rs2244526	>0.05
SERPINB1(dist=1531), MIR4645(dist=10653)	rs398312	>0.05
SFTPB	rs1130866	0.0204
STAU1	rs6066975	>0.05
TSPAN5	rs1918742	>0.05

TT was an independent risk factor for severe disease (OR=3.447, 95% CI=1.421-8.361, P=0.006). In addition, rs6487132-GG or rs6487132-AG was also overrepresented in patients with severe disease than in patients with mild disease (15.9% [14/88] vs 6.8% [12/165], P=0.019; OR=2.601, 95% CI=1.148-5.897). Multivariate analysis showed that rs7314545-CT or rs7314545-TT and rs6487132-GG or rs6487132-AG were independent risk factors for severe disease (OR=3.447, 95% CI=1.421-8.361, P=0.006).

In vitro viral replication study showed that siRNA-mediated knockdown of PDE3A expression in A549 cells significantly enhanced the replication of A(H1N1)pdm09 virus (Fig).

Discussion

Comparing the genotypes between patients with severe and mild A(H1N1)pdm09 virus infection, we showed that SNPs in the *SFTPB* gene (rs1130866) and *PDE3A* gene (rs6487132 and rs7314545) were associated with disease severity. Multivariate analysis showed that these SNPs were independent risk factors for severe influenza. In vitro studies confirmed that *SFTPB* and *PDE3A* are related to virus replication. Therefore, we successfully identified host factors that play a role in the innate immunity against influenza virus infection.

Surfactant is present in the alveoli, and is important in lowering the surface tension, thereby avoiding the collapse of the alveoli. There are four surfactant proteins, including SP-A, SP-B, SP-C, and SP-D. Previous studies showed that SP-A and SP-D possess antiviral activity against influenza virus. Our study showed that SP-B can also inhibit the replication of influenza viruses.

Phosphodiesterase (PDE) regulates the concentration of the intracellular second messengers cyclic adenosine monophosphate and cyclic guanosine monophosphate, thereby regulating many physiological functions. Regarding virus infections, inhibition of PDE4 by rolipram improved

TABLE 2. Comparison of the rs1130866 genotypes between patients with laboratory-confirmed A(H1N1)pdm09 infection or A(H3N2) infection and in the general Han Chinese population

	CC genotype, No (%)		Odds ratio (95% confidence interval)	P value (Fisher's exact test)
	Different patient groups	General Han Chinese population (n=197)		
Recessive model				
Severe A(H1N1)pdm09 (n=153)	116 (75.8)	97 (49.2)	3.232 (2.033-5.139)	5.60×10^{-7}
All A(H1N1)pdm09 (n=380)	248 (65.3)	97 (49.2)	1.937 (1.365-2.749)	2.37×10^{-4}
Dominant model				
Severe A(H1N1)pdm09 (n=153)	151 (98.7)	182 (92.4)	6.223 (1.401-27.640)	0.006
All A(H1N1)pdm09 (n=380)	369 (97.1)	182 (92.4)	2.765 (1.245-6.141)	0.018

the survival of mice infected with influenza A virus. Polymorphism of PDE8A is associated with HIV-1 replication in primary macrophages. Our study demonstrated that knockdown of *PDE3A* enhanced viral replication, suggesting that PDE3A is an antiviral host factor. We identified that *SFTPB* and *PDE3A* were important susceptibility genes for severe A(H1N1) infection in our population. Together with other susceptibility genes identified to be important for influenza virus infections in humans, we may be able to build a model for predicting prognosis of a patient with influenza virus infection.[1] *SFTPB* and *PDE3A* are involved in the pathogenesis of A(H1N1) pdm09 infection, and additional work on these genes and influenza virus infection may be useful in identifying host- directed antivirals for the treatment of influenza virus infection.

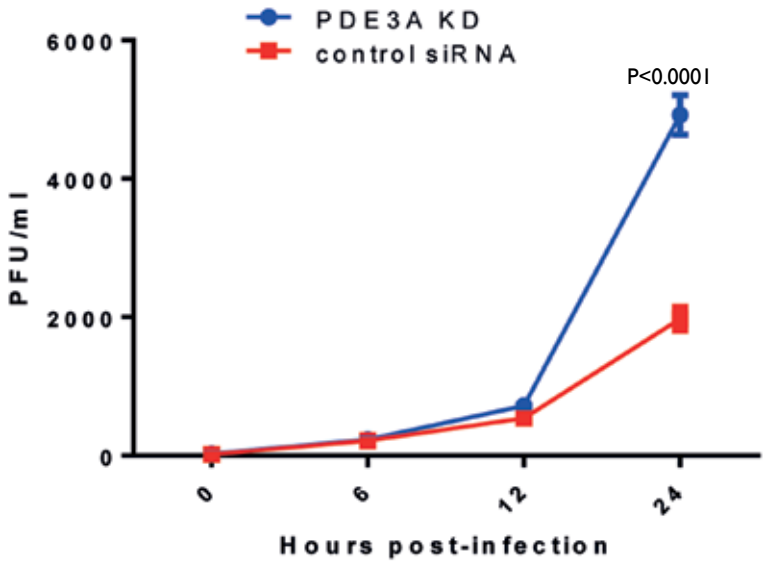

FIG. Effect of PDE3A KD compared with control siRNA on A(H1N1)pdm09 virus replication in A549 cells. A549 cells were transfected with PDE3A-specific siRNA or control siRNA. PDE3A mRNA expression was lowered by >80% at all time points for PDE3A KD cells when compared with cells transfected with control siRNA. A549 cells were infected with A/HK/415742/2009 (H1N1) virus at an MOI of 0.1.

Conclusion

SFTPB and *PDE3A* are independent host susceptibility genes for severe influenza A(H1N1) pdm09 virus infection for the Chinese population in Hong Kong.

Acknowledgements

This study was supported by the Health and Medical Research Fund, Food and Health Bureau, Hong Kong SAR Government (#13120842). We are grateful for the support from the Centre for Genomic Sciences, The University of Hong Kong.

Results from this study have been published in:

(1) To KKW, Zhou J, Song YQ, et al. Surfactant protein B gene polymorphism is associated with severe influenza. Chest 2014;145:1237-43.

(2) To KK, Zhou J, Chan JF, Yuen KY. Host genes and influenza pathogenesis in humans: an emerging paradigm. Curr Opin Virol 2015;14:7-15.

References

1. To KK, Zhou J, Chan JF, Yuen KY. Host genes and influenza pathogenesis in humans: an emerging paradigm. Curr Opin Virol 2015;14:7-15.
2. Ding B, Abe JI, Wei H, et al. Functional role of phosphodiesterase 3 in cardiomyocyte apoptosis: implication in heart failure. Circulation 2005;111:2469-76.

B-1 cell response and its regulation during influenza virus infection

L Lu *, X Wang, K Ma, M Chen, KH Ko, BJ Zheng

KEY MESSAGES

1. Pleural cavity B-1a cells rapidly infiltrate lungs during influenza infection.
2. Pulmonary B-1a cells produce natural antibodies as first-line protection against influenza lung infection.
3. IL-17A deficiency impairs natural antibody production by B-1a cells.
4. IL-17A promotes B-1a cell differentiation into high-rate IgM producing cells in lung tissue.

Hong Kong Med J 2019;25(Suppl 7):S30-2
HMRF project number: 13121202

L Lu, X Wang, K Ma, M Chen, KH Ko, BJ Zheng

Department of Pathology and Centre of Infection and Immunology, The University of Hong Kong

* Principal applicant and corresponding author: liweilu@hku.hk

Introduction

Outbreaks of influenza infection are a threat to public health in Hong Kong. Influenza infection is generally localised in the respiratory tract where virus-binding antibodies provided by B cells are essential for antiviral immune response against influenza infections by opsonisation of pathogens and activation of complement receptor-mediated phagocytosis. During influenza infection, virus-binding antibodies are produced by two sources, B-1 cells and conventional B-2 cells. Owing to low frequency of viral antigen-specific B-2 cells at the onset of infection, early induction of natural antibody response by B-1 cells becomes critical for immune protection against influenza infection. Although natural IgM antibodies produced by B-1 cells have been recognised to provide the first-line protection by directly neutralising influenza virus,[1-5] it remains unclear what molecular mechanisms regulate this process.

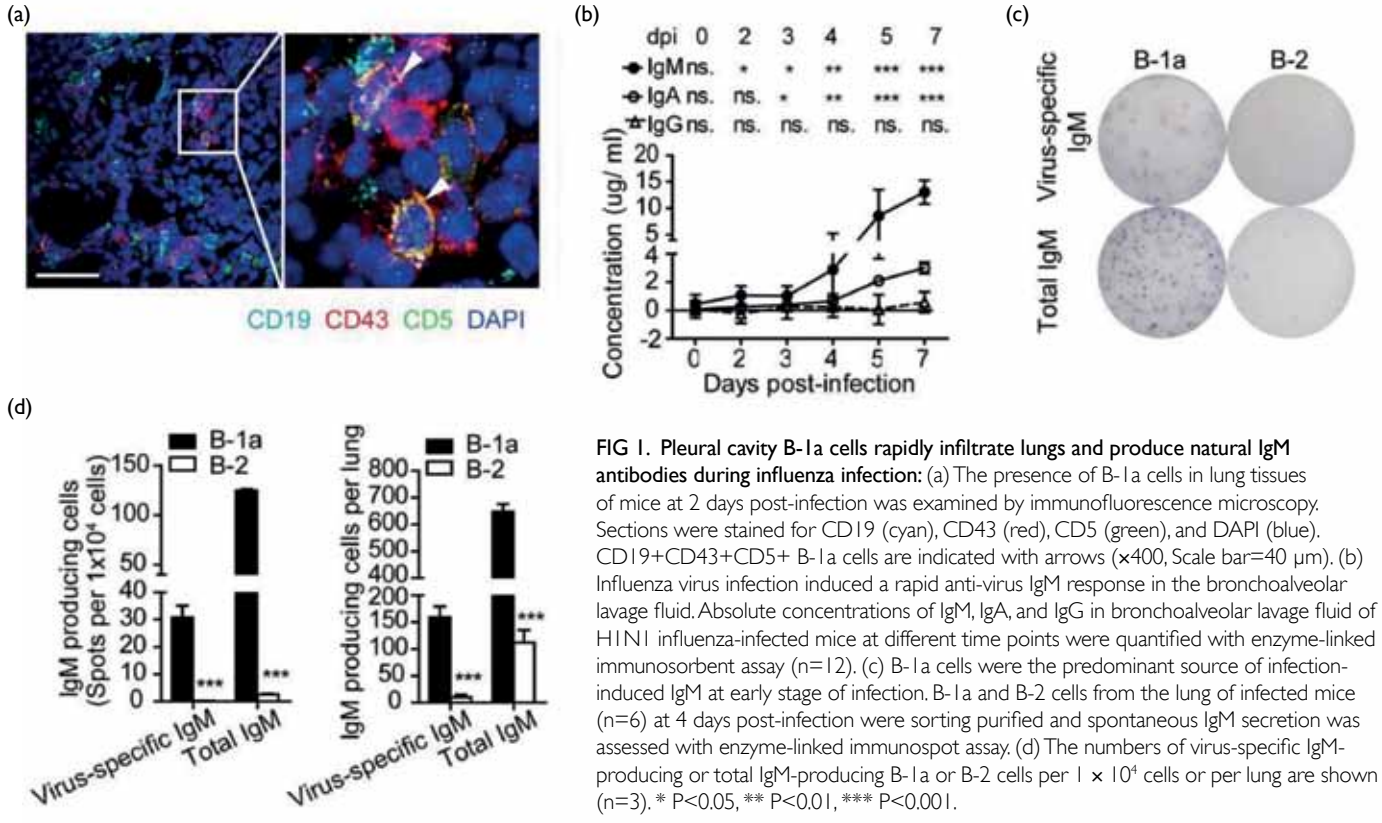

FIG 1. Pleural cavity B-1a cells rapidly infiltrate lungs and produce natural IgM antibodies during influenza infection: (a) The presence of B-1a cells in lung tissues of mice at 2 days post-infection was examined by immunofluorescence microscopy. Sections were stained for CD19 (cyan), CD43 (red), CD5 (green), and DAPI (blue). CD19+CD43+CD5+ B-1a cells are indicated with arrows (×400, Scale bar=40 μm). (b) Influenza virus infection induced a rapid anti-virus IgM response in the bronchoalveolar lavage fluid. Absolute concentrations of IgM, IgA, and IgG in bronchoalveolar lavage fluid of H1N1 influenza-infected mice at different time points were quantified with enzyme-linked immunosorbent assay (n=12). (c) B-1a cells were the predominant source of infection-induced IgM at early stage of infection. B-1a and B-2 cells from the lung of infected mice (n=6) at 4 days post-infection were sorting purified and spontaneous IgM secretion was assessed with enzyme-linked immunospot assay. (d) The numbers of virus-specific IgM-producing or total IgM-producing B-1a or B-2 cells per 1×10^4 cells or per lung are shown (n=3). * P<0.05, ** P<0.01, *** P<0.001.

Results and discussion

We discovered that airway exposure to influenza caused migration of B-1a cells, a subset of B-1 cells, to the lung tissue in infected mice. Lung-infiltrating B-1a cells underwent further differentiation into plasma cells with enhanced production of protective natural IgM antibodies (Fig 1). As an important cytokine locally induced by influenza virus infection, IL-17A critically regulated this process by driving B-1a cell differentiation into high-rate IgM producing plasma cells in the lung tissue during influenza infection. Notably, deficiency of IL-17A led to reduced production of virus-binding natural antibodies by B-1 cells. Furthermore, we elucidated the molecular mechanisms by which IL-17A activates Blimp-1 gene expression and promotes B-1 cell differentiation into plasma cells for natural antibody production (Fig 2). Together, these results

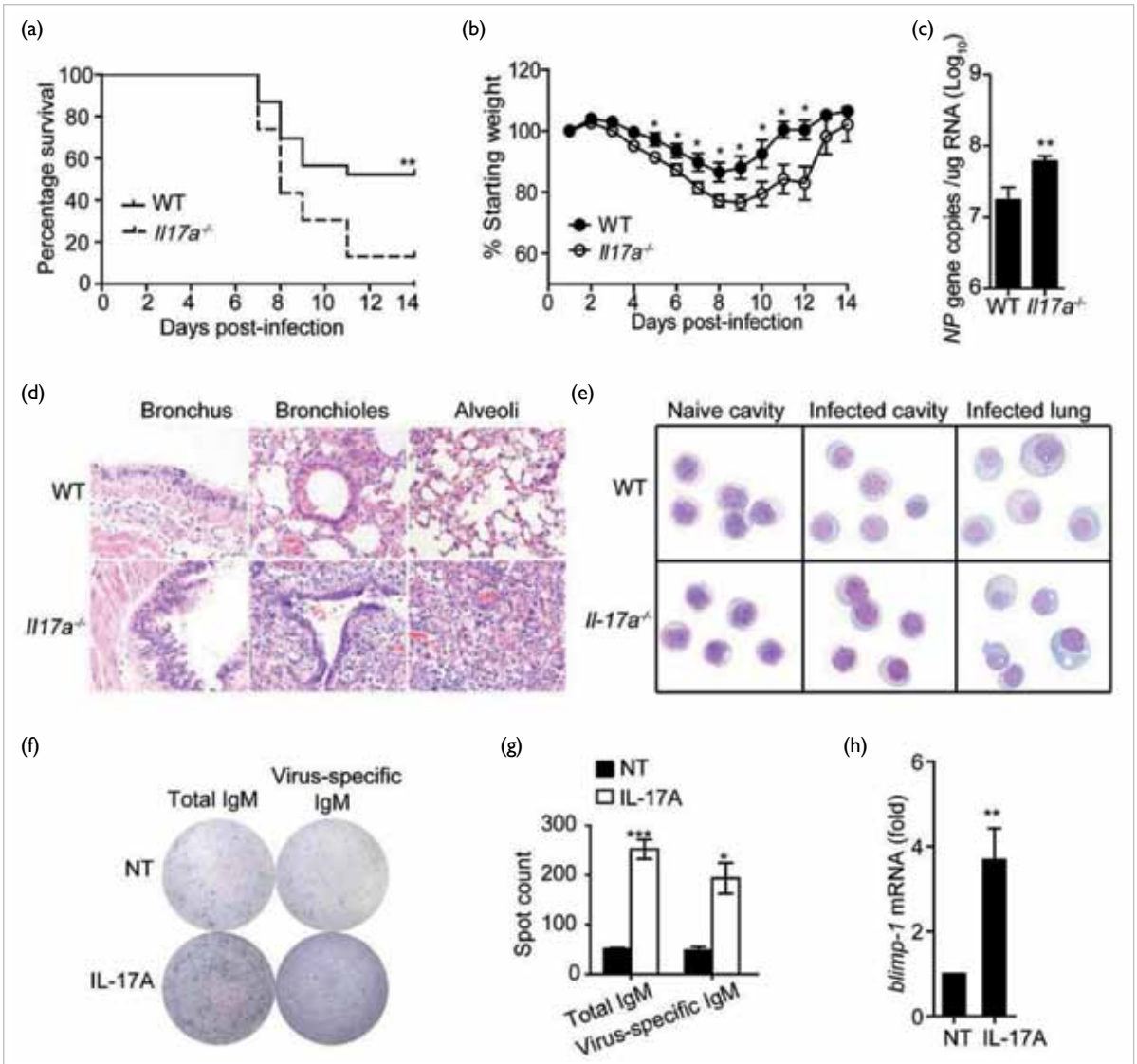

FIG 2. IL-17A promotes B-1a cell differentiation into high-rate IgM producing cells by activating *blimp-1* gene expression: (a, b) H1N1 influenza virus-infected IL-17A deficient (*Il17a*$^{-/-}$) mice exhibited significantly reduced survival rate and body weight compared with wild-type control mice (n=23). (c) The copy number of influenza virus NP gene in the lung tissues at 5 days post-infection was measured by quantitative real-time PCR. The *Il17a*$^{-/-}$ mice exhibited a much higher viral burden than wild-type controls (n=6). (d) Histological analysis revealed substantially increased severity of lung damage in *Il17a*$^{-/-}$ mice, characterised by pronounced inflammatory destruction and leukocyte infiltration at 5 days post-infection following challenge with influenza virus (×200). (e) Morphology of B-1a cells from the pleural cavity of naïve mice or pleural cavity and lung tissues of H1N1-infected wild-type and *Il17a*$^{-/-}$ mice at 5 days post-infection was examined by cytospin preparation and Wright's staining. B-1a cells from lung tissue of infected *Il17a*$^{-/-}$ mice showed morphologically reduced differentiation level. (f, g) B-1a cells were sorting-purified from pleural cavity of wild-type mice and cultured with or without recombinant murine IL-17A (rmIL-17A) (20 ng/ mL) for 5 days. Production of total IgM and virus-specific IgM in supernatants of cultured B-1a cells was examined with enzyme-linked immunospot assay. (h) Sorting purified B-1a cells from pleural cavity of wild-type mice were cultured with or without rmIL-17A (20 ng/ mL) for 24 hours. Real-time PCR analysis showed that IL-17A promoted blimp-1 gene expression in B-1a cells. * P<0.05, ** P<0.01, *** P<0.001.

have demonstrated that IL-17A is a key factor that modulates natural antibody production by B-1 cells in the lung during influenza infection.

These findings provide new insights in understanding how natural antibody production by B-1 cells is regulated by IL-17A, an important process in early immune response against influenza infection. This study will facilitate further investigations to validate IL-17A as an immune stimulator in designing effective vaccines for preventing influenza infection in human. We will further study the functional modulation of B-1 cell response and develop a new strategy by targeting B-1 cells for the effective treatment of influenza infection.

Acknowledgements

This study was supported by the Health and Medical Research Fund, Food and Health Bureau, Hong Kong SAR Government (#13121202). We thank Dr Yoichiro Iwakura (The University of Tokyo) for providing Il17a$^{-/-}$ mice. We also thank the technical support from the Laboratory Animal Unit and Medical Faculty Core Facility at the University of Hong Kong.

Results of this study have been published in: Wang X, Ma K, Chen M, Ko KH, Zheng BJ, Lu L. IL-17A promotes pulmonary B-1a cell differentiation via induction of blimp-1 expression during influenza virus infection. PLoS Pathog 2016;12:e1005367.

References

1. Hayakawa K, Hardy RR, Honda M, Herzenberg LA, Steinberg AD, Herzenberg LA. Ly-1 B cells: functionally distinct lymphocytes that secrete IgM autoantibodies. Proc Natl Acad Sci U S A 1984;81:2494-8.
2. Ha SA, Tsuji M, Suzuki K, et al. Regulation of B1 cell migration by signals through Toll-like receptors. J Exp Med 2006;203:2541-50.
3. Berberich S, Forster R, Pabst O. The peritoneal micromilieu commits B cells to home to body cavities and the small intestine. Blood 2007;109:4627-34.
4. Baumgarth N, Herman OC, Jager GC, Brown L, Herzenberg LA, Herzenberg LA. Innate and acquired humoral immunities to influenza virus are mediated by distinct arms of the immune system. Proc Natl Acad Sci U S A 1999;96:2250-5.
5. Choi YS, Baumgarth N. Dual role for B-1a cells in immunity to influenza virus infection. J Exp Med 2008;205:3053-64.

Vaccine-induced T cell protection from influenza viruses

SA Valkenburg *, OTW Li, JSM Peiris, LP Perera, LLM Poon

KEY MESSAGES

1. T cell–activating vaccines provide robust protection against diverse influenza viruses, which is not possible by current inactivated influenza vaccines.
2. Wyeth/IL-15/5flu is a universal anti-influenza vaccine.
3. CD4 and CD8 T cells act together for protection from influenza viruses.

Hong Kong Med J 2019;25(Suppl 7):S33-6
HMRF project number: 13121142

[1] **SA Valkenburg, [1] OTW Li, [1] JSM Peiris, [2] LP Perera, [1] LLM Poon**

[1] *Centre of Influenza Research and School of Public Health, The University of Hong Kong, Hong Kong*
[2] *Metabolism Branch, Center for Cancer Research, National Cancer Institute, NIH, Bethesda, MD, USA*

* Principal applicant and corresponding author: sophiev@hku.hk

Introduction

Influenza causes yearly seasonal epidemics, worldwide pandemics, and occasional outbreaks from cross species transmission, despite availability of vaccines and antiviral drugs. A diverse array of influenza viruses circulates between different species, reassort and drift antigenically over time, yet certain immune targets remain relatively constant across diverse strains of influenza viruses.[1] Vaccines that target such conserved regions enable universal immunity against influenza. It is essential to improve influenza vaccines to provide broadly reactive immune protection from pandemic and outbreak influenza viruses to pre-arm the immune system. Virus-specific $CD4^+$ and $CD8^+$ T cells responses kill virus-infected cells, coordinate local innate immune responses, and react against different strains and subtypes of influenza secondary to conservation of immune targets. A vaccine designed to stimulate T cell immunity towards heterosubtypic strains of influenza is generated.[2] This multivalent vaccinia virus-based H5N1 influenza vaccine (Wyeth/IL-15/5flu) expresses five H5N1-derived influenza proteins (HA, NA, M1, M2, and NP), in combination with the immune stimulatory cytokine interleukin-15 (IL-15).[2] We assessed the breadth of immunity generated by the vaccine in a mouse model with challenge of seasonal, pandemic, and highly lethal avian influenza viruses.[3] Vaccinated mediated protection was dependent on T cell recruitment, especially engagement of CD4 T cells, as a cornerstone of the vaccine immune response.

Methods

Vaccination and infection of mice

Female BALB/c ($H\text{-}2^d$) mice (6-8 weeks of age) were primed twice 3 weeks apart via the subcutaneous route with 10^7 plaque-forming units in 100 μL PBS of vaccinia Wyeth/IL-15/5flu, Wyeth/mutIL-15/5flu, Wyeth, or PBS alone, and then challenged with influenza virus 3 weeks later. For influenza challenge, mice were anaesthetised and infected intranasally with 25 μL of H7N9 (A/Shanghai/2/2013), HPAI H7N7 (A/Netherlands/219/2003), mouse-adapted H3N2 (A/Hong Kong/1/68-MA20C), or pandemic H1N1 (A/California/04/2009). All experiments involving H7N9 and HPAI H7N7 viruses were conducted in a BSL3 laboratory. All animal studies were approved by the institutional animal ethics committee. Mice were monitored for survival, weight loss, and symptom severity (n=5 per group). Infected lungs were harvested at day 7 (n=3) for viral loads by standard TCID50 assay on MDCK cells.

Intracellular cytokine staining for influenza-specific T cells

Lymphocytes from vaccinated mice or human PBMC (resting or restimulated with vaccine) were stimulated in vitro with low pathogenic H5N2 virus (to represent vaccine-specific T cell responses) for 6 hours and then in the presence of BFA for 12 hours. CD4 and CD8 T cell IFNγ accumulation was measured by intracellular cytokine staining and flow cytometry.

Selective depletion of T cell subsets

Vaccinated mice were depleted of $CD4^+$ T cells, $CD8^+$ T cells, or both prior to influenza infection. Mice were treated with GK1.5 (anti-CD4) and 2.43 (anti-CD8) or isotype control (IgG2b) monoclonal antibodies (BioXCell) at 100 μg intraperitoneally at days -4, -2, 0, and 3.[4] Depletion was confirmed at day -1 at >98%, compared with isotype-treated mice and non-depleted mice. Untouched magnetically purified CD4 or CD8 T cells were isolated from

the spleens of naïve mice by MagCellect kit (R&D). Naïve T cells (1×10^6 cells per mouse) were given intravenously to T cell–depleted recipient BALB/c as indicated (Fig 2). Mice were then challenged with H3N2. Mice were monitored for survival, weight loss, and symptom severity (n=5 per group). Infected lungs were harvested at day 7 (n=3) for viral loads by standard TCID50 assay on MDCK cells.

PBMC vaccine restimulation

Human PBMCs were isolated from Red Cross buffy packs by density gradient centrifugation and stored in liquid nitrogen. PBMCs were restimulated with ultraviolet-inactivated Wyeth/IL-15/5flu virus for 10 days in vitro in the presence of IL-2 (10U/mL). At day 10, matching un-restimulated PBMCs from the same donors were used for baseline comparisons. CD4 and CD8 T cell IFNγ production was assessed by intracellular cytokine staining following stimulation with Wyeth/IL-15/5flu, Wyeth, H5N2 viruses (MOI 2) or PBS. Samples were acquired by flow cytometry.

Results

Wyeth/IL-15/5flu, a live replicating vaccinia virus encoding five H5N1-derived influenza proteins and IL-15 cytokine as a molecular adjuvant, is a robust universal anti-influenza vaccine. Lethal influenza challenge of vaccinated BALB/c (Fig 1) and B6 mice (data not shown) had 100% survival, whereas unvaccinated mice all succumbed to infection. Increased survival of vaccinated mice was accompanied by reduced peak viral loads at day 3 (data not shown), early viral clearance by day 7 after infection, improved weight recovery, and reduced symptom severity.

Protection of vaccinated mice correlated with significantly elevated cross-reactive H5-specific T cells at the site of infection. Influenza-specific CD4 and CD8 T cells were substantially increased in the lungs, spleen, and lymph nodes of vaccinated mice. Passive transfer of T cell subsets from vaccinated mice to naïve recipient mice showed reduced viral loads and increased survival (data not shown), whereas serum transfer was unable to confer any level of protection. Therefore, to determine the contribution of T cell subsets to vaccine-mediated protection, selective depletion of T cell subsets was performed at the time of vaccination or challenge in combination with naïve T cell transfer (Fig 2).

Despite CD8 T cells having a role in protection from influenza infection, our vaccine continued to

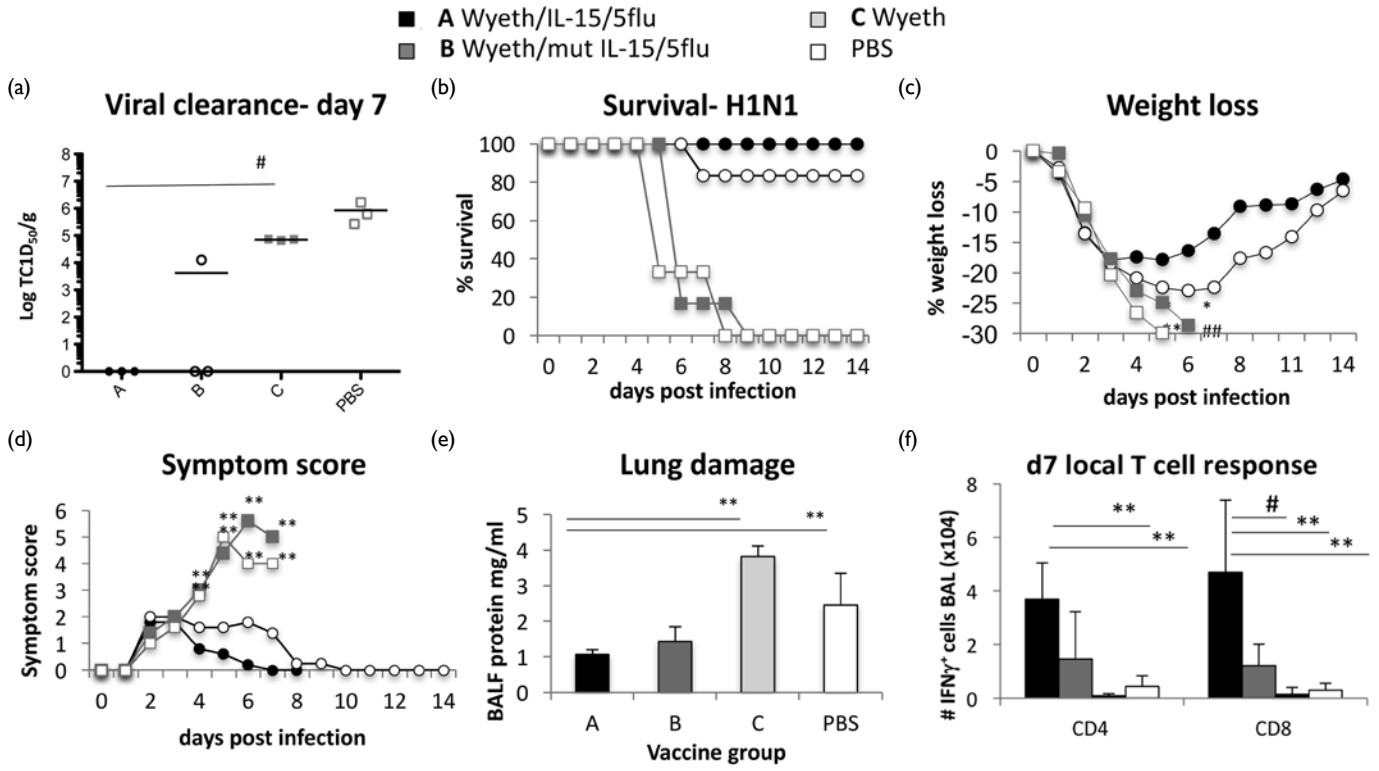

FIG 1. Wyeth/IL-15/5flu reduces viral load, morbidity, and mortality against heterologous challenge. BALB/c mice were vaccinated with Wyeth/IL-15/5flu, Wyeth/mut-IL-15/5flu, Wyeth (control vaccine vector), or PBS twice 3 weeks apart and then challenged with H7N9, H7N7, H3N2, or H1N1. (a) Lung viral titres by standard MDCK TCID50 assay (H3N2) at day 7. Mice were monitored daily for (b) survival, (c) weight loss, and (d) symptoms of H1N1 influenza infection. (e) Lung damage was assessed by total protein concentration in the BAL in a standard BCA assay. (f) Cells isolated by BAL wash of the lungs from day 7 after H3N2 infection were stimulated H5N2 virus (MOI2) for 6 hours, and 12 hours with BFA. IFNγ production by CD4 and CD8 T cells was assessed by ICS and samples acquired by flow cytometry. # P<0.05, * P<0.01, ## P<0.005, ** P<0.001 versus A vaccine group.

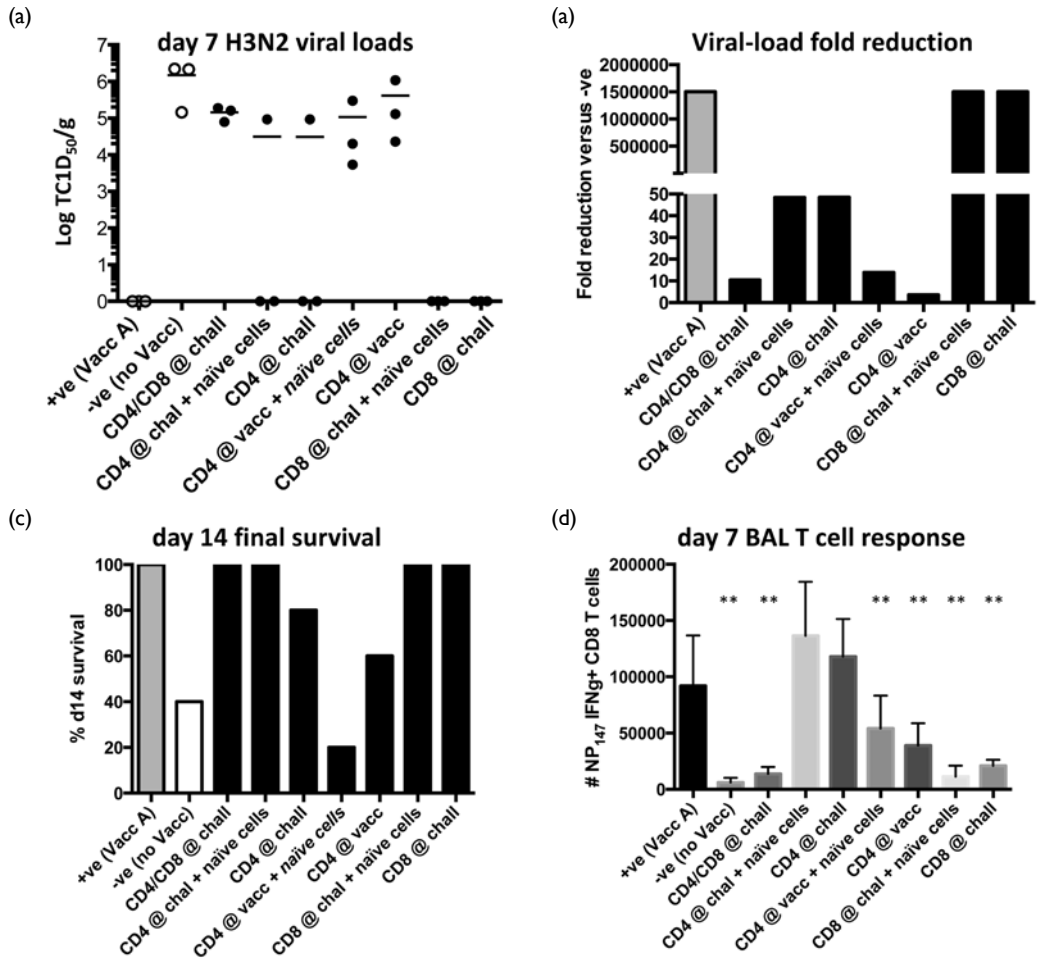

FIG 2. T cell depletion impairs CD4 help for memory and CD4 T cells are needed at challenge for protection. Mice were depleted for CD4+CD8 at challenge, CD4 at challenge or vaccination, or CD8 at challenge. Prior to infection, selected mice were given naïve splenocytes intravenously (10 days after the final depletion). Mice were infected with H3N2. (a) Lung viral load was determined at day 7 (n=3). (b) Fold reduction in viral load was compared with negative controls, and (c) monitored for survival at day 14 (n=5). (d) BAL NP147-specific CD8 T cells were enumerated from day 7 after H3N2 infection (n=3).

confer protection in CD8 depleted mice. Conversely, CD4 and CD4+CD8 depletion at the time of challenge had elevated viral loads and reduced survival (Fig 2). However, depletion of CD4 T cell subsets at the time of vaccination impaired the formation of CD8 T cell memory and resulted in further increased viral loads. CD4 and CD8 T cells act in synergy for vaccine-mediated protection, and CD4 T cells are essential for protection.

Our vaccine was universally immunostimulatory, providing protection in different mouse strains, reduced viral loads in immune-compromised nude and SCID mice (data not shown), and further stimulated human PBMCs to generate increased H5-specific CD4 T cell responses in vitro (Fig 3). Restimulation of human PBMCs with ultraviolet-inactivated Wyeth/IL-15/5flu resulted in proliferation and expansion of vaccinia-specific and H5-specific T cells, especially H5-specific CD4 T cells, which showed a significant increase from baseline memory levels in paired uncultured samples.

Discussion

T cell–activating vaccines are broadly protective against influenza infection and are a promising approach for clinical development. The breadth of T cell–mediated vaccine protection covered diverse strains, subtypes, and highly lethal avian influenza viruses. T cells from vaccinated mice were necessary for protection from influenza infection, especially CD4 T cells for their helper functions formation of CD8 T cell memory and antibodies; however, CD4 T cells themselves were necessary at the time of vaccination to mediate protection from lethal infection. New roles are emerging of the pivotal roles of CD4 T cells play during vaccination and infection responses.[5]

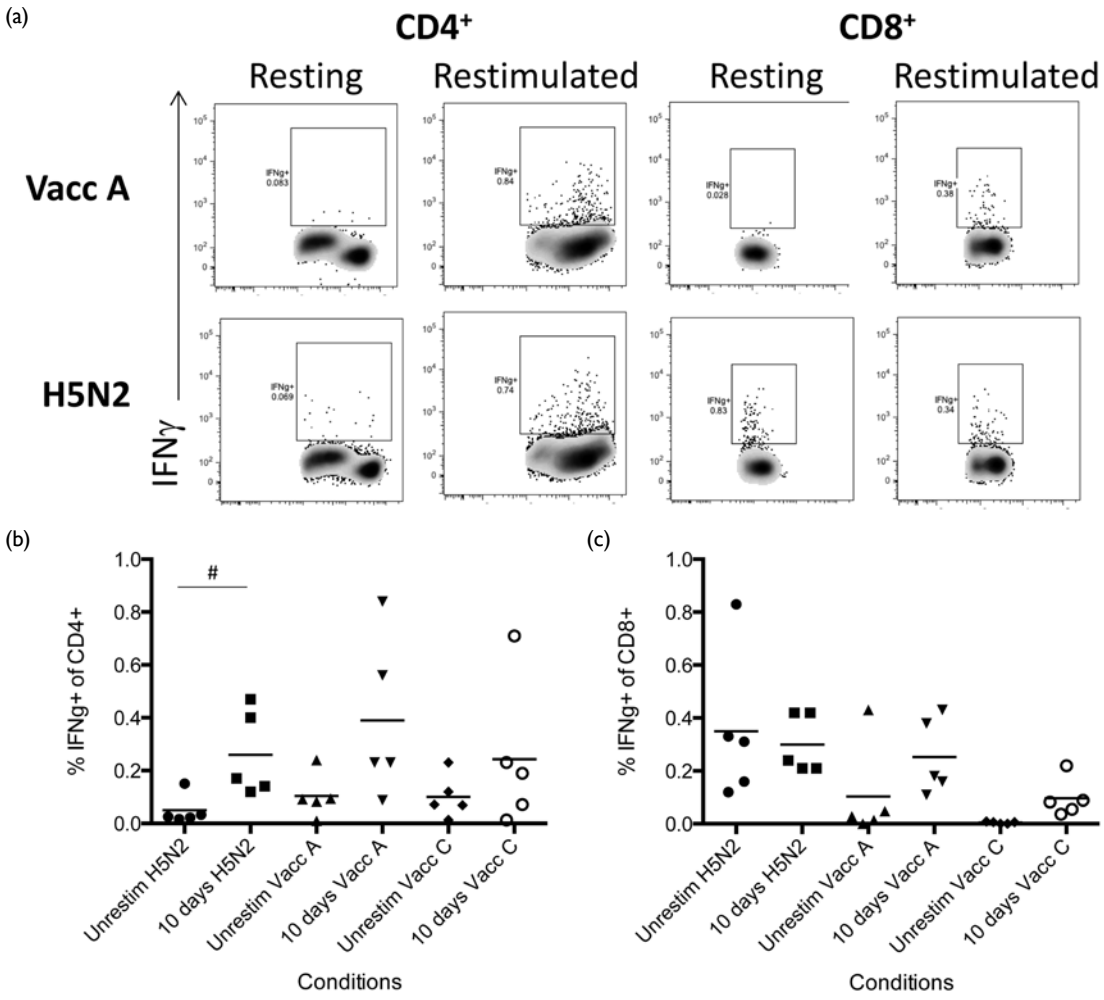

FIG 3. Human PBMCs restimulated with vaccinia A have increased H5-specific CD4+ T cells. PBMCs (n=5 donors) were restimulated with ultraviolet-inactivated vaccinia A virus for 10 days in the presence of IL-2. At day 10, cells were stimulated with H5N2 (MOI4), Wyeth/IL-15/5flu, Wyeth, or PBS (negative control). Direct ex vivo restimulation of resting CD4 and CD8 T cells from matched donors was also performed. CD4 and CD8 T cells were assessed for IFNγ production by intracellular cytokine staining. (a) Representative FACS plots of IFNγ CD4 and CD8+ T cells, (b) Individual donors CD4 T cells, and (c) CD8 T cells.

Acknowledgement

This study was supported by the Health and Medical Research Fund, Food and Health Bureau, Hong Kong SAR Government (#13121142).

Results from this study have been published in:
(1) Valkenburg SA, Li OT, Mak PW, et al. IL-15 adjuvanted multivalent vaccinia-based universal influenza vaccine requires CD4+ T cells for heterosubtypic protection. Proc Natl Acad Sci U S A 2014;111:5676-81.
(2) Valkenburg SA, Li OTW, Li A, et al. Protection by universal influenza vaccine is mediated by memory CD4 T cells. Vaccine 2018;36:4198-206.

References

1. Assarsson E, Bui HH, Sidney J, et al. Immunomic analysis of the repertoire of T-cell specificities for influenza A virus in humans. J Virol 2008;82:12241-51.
2. Poon LL, Leung YH, Nicholls JM, et al. Vaccinia virus-based multivalent H5N1 avian influenza vaccines adjuvanted with IL-15 confer sterile cross-clade protection in mice. J Immunol 2009;182:3063-71.
3. Valkenburg SA, Li OT, Mak PW, et al. IL-15 adjuvanted multivalent vaccinia-based universal influenza vaccine requires CD4+ T cells for heterosubtypic protection. Proc Natl Acad Sci U S A 2014;111:5676-81.
4. Guo H, Santiago F, Lambert K, Takimoto T, Topham DJ. T cell-mediated protection against lethal 2009 pandemic H1N1 influenza virus infection in a mouse model. J Virol 2011;85:448-55.
5. McKinstry KK, Strutt TM, Kuang Y, et al. Memory CD4+ T cells protect against influenza through multiple synergizing mechanisms. J Clin Invest 2012;122:2847-56.

Transfer of HIV-1 from HIV-1 latently infected CD34+ haematopoietic progenitors to CD4+ T cells

AKL Cheung *, Y Huang, M Chen, ZW Chen

KEY MESSAGES

1. HIV-1 can infect CD34+ progenitor stem cells and become latent.
2. Latent HIV-1 can affect the CD34 cell to halt homeostasis.
3. HIV-1–infected CD34+ progenitors may be a vehicle for viral dissemination.

Hong Kong Med J 2019;25(Suppl 7):S37-40
HMRF project number: 13120612

AKL Cheung, Y Huang, M Chen, ZW Chen

AIDS Institute, Department of Microbiology, LKS Faculty of Medicine, The University of Hong Kong

* Principal applicant and corresponding author: akcheung@hkbu.edu.hk

Introduction

It remains controversial whether HIV-1 can infect CD34+ haematopoietic stem cells in the human host. HIV-1 can establish a latent reservoir in vitro and in vivo. This study aims to elaborate on latency of HIV-1 infection in CD34+ haematopoietic stem cells. During latency, HIV-1 remains quiescent and viral replication is very limited with no consequence of immune clearance with declining CD4 counts. Although activation of memory CD4 T cells leads to HIV replication, this does not occur in detectable levels during the latency phase of HIV infection. Latency in the primary site CD4+ T cells can occur within 1 week after primary infection. However, attempts to purge latency have not been successful, despite using different agents to reactivate latent HIV-1 genome in CD4+ T cells.[1] Nonetheless, HIV-1 genome is preferentially present in long-lasting central memory CD4+ T cells and T cells with stem cell-like properties.[2] Latency in CD4+ T cells has been reported,[3] but CD34+ haematopoietic progenitor as a latent reservoir of HIV remains poorly understood.[4] These progenitor cells can be latently infected by HIV-1 without active virus production unless reactivation is induced. Furthermore, in HIV-1 patients, 0.025% to 0.4% of integrated HIV-1 genome is found in CD34+ cells in the bone marrow. The underlying mechanism and how HIV-1 modulated immune response in CD34+ progenitor cells after latent infection remains elusive.

Methods

Healthy human peripheral blood mononuclear cells (PBMCs) were isolated from buffy coats obtained from Hong Kong Red Cross, and 2×10^8 PBMCs were used for magnetic bead separation and cultured in StemPro34 serum-free media (Invitrogen) with 25 ng/mL GM-CSF, 100 ng/mL SCF, 50 ng/mL IL-3 (Peprotech) at a density of 2×10^4 cells/0.2 mL per well in a U-bottom 96-well culture plate for up to 14 days with one-third media change every 3-4 days.

HIV-1 viruses (strains NL4-3 and JRFL) were propagated using PHA/IL2-activated healthy human PBMCs, and virus titre was assessed using p24 ELISA kit according to manufacturer instructions (ZeptoMatrix). HIV-1 infection was performed using 20-50 ng p24 per mL per 5×10^6 cells. To construct pseudoviruses, Red-Green-HIV (RGH) plasmid and plasmid-encoding envelope proteins from X4-tropic HxB2 (ie, X4-RGH) and R5-tropic JR-FL (R5-RGH) were used to co-transfect 293T cells. After 2 days, supernatants were collected and virus concentrated by ultracentrifugation against sucrose gradient. Infected cells were monitored for fluorescent signals using confocal microscopy.

Digital PCR was performed using primers and probes described previously[5] in the QuantoStudio 3D digital PCR system or ViiA7 real-time PCR instrument (Life Technologies). Flow cytometry was performed to examine the expression of HLA-DR, HLA-A,B,C, CD4, CD34, CD33, and p24 (KC57; Becton Dickinson).

Results

HIV-1 infection of PB-CD34 cells

We performed a series of experiment including qPCR, dPCR, and p24 detection to determine if HIV-1 can infect PB-CD34 cells. First, we analysed HIV-1 integration into PB-CD34 cell genome. To increase the sensitivity of detection of proviral HIV-1 DNA, we conducted the TaqMan assay using digital PCR (QS3D, Life Technologies) that allows absolute quantification of DNA copy number without a reference gene. To accurately determine the number of host DNA copies found in the input template, we further used the CCR5 assay.[5] Combing the results,

we found that in 500 cells, there were approximately 25 copies of proviral HIV-1 DNA (~5% infection) in X4- or R5-tropic virus infection of PB-CD34 cells (Fig 1).

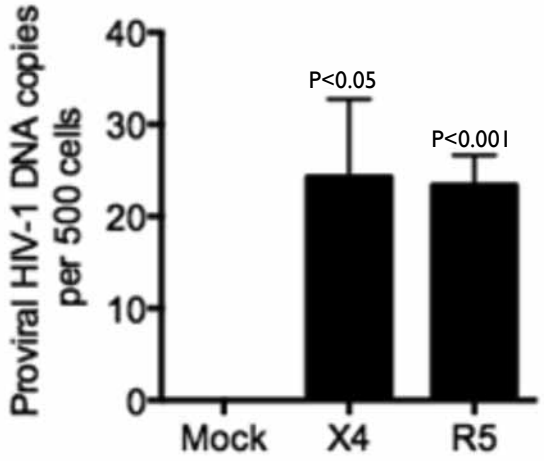

FIG 1. DNA copy number in HIV-1 infection of PB-CD34 cells: At day 1 following mock, X4-tropic, or R5-tropic HIV-1 live virus infection, cells were harvested for DNA extraction. TaqMan assays were performed for dPCR for HIV-1 p17. qPCR for CCR5 was performed to determine number of cells in the template.

Dual-reporter pseudovirus infection of PB-CD34 cells

To further illustrate that PB-CD34 cells can support HIV-1 infection, we used the dual reporter construct RGH. RGH differentiates between silent latent infection and active infection based on Gag-eGFP (green) and Nef-mCherry (pink) fluorescences, such that early eGFP detection indicates active infection, mCherry indicates latent infection, and dual positive represented by co-localised yellow fluorescence depicts *de novo* Gag expression and integrated latent virus (Fig 2a). Pseudoviruses with X4-tropic HxB2 (X4-RGH) and R5-tropic JR-FL (R5-RGH) envelopes were generated. The infectious ability of the RGH pseudovirus was first tested in GHOST(3)-CXCR4$^+$CCR5$^+$ cells. At day 2 post-infection, eGFP and mCherry signals can be detected on GHOST cells and some cells have co-localised signals (yellow arrows) [Fig 2b], suggesting that integration and replication can be detected using X4-RGH. Similar results were obtained for R5-RGH (data not shown) and validates that the pseudoviruses generated can be used. Next, PB-CD34 cells were infected with X4- or R5-RGH pseudoviruses. After 2 days, confocal microscopy was used to determine fluorescence signals. PB-CD34 cells infected with X4- or

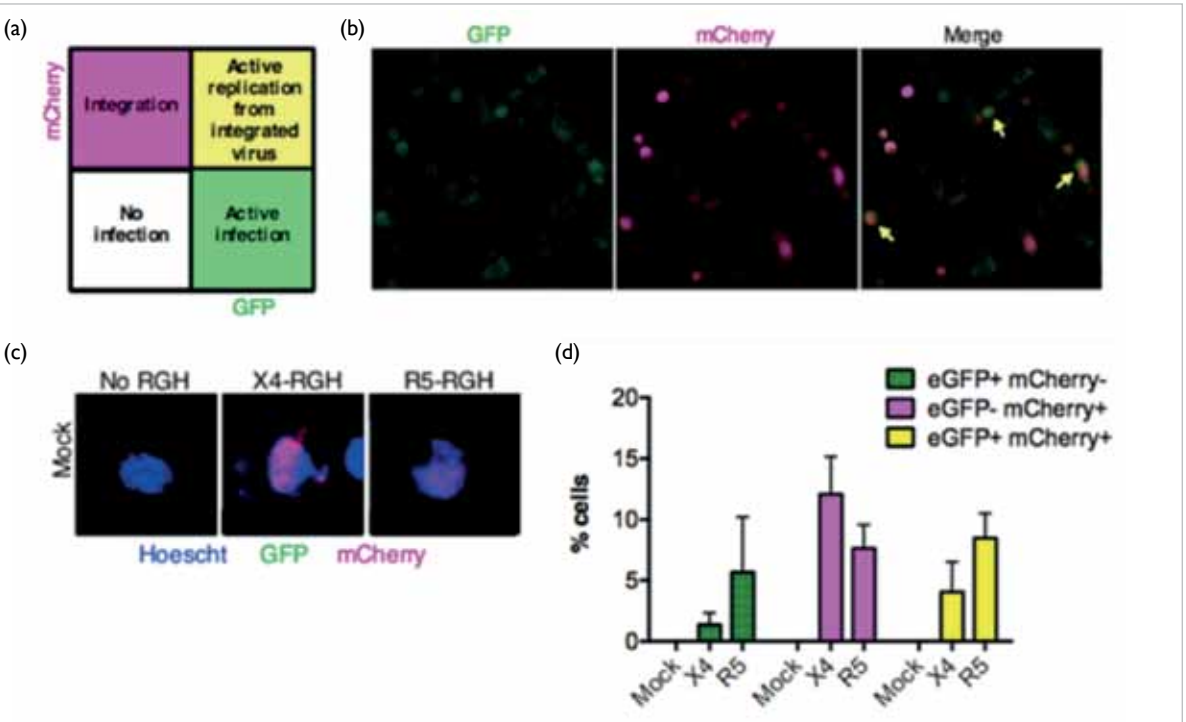

FIG 2. HIV-1 integration and infection of PB-CD34 cells using a dual-reporter pseudovirus: Pseudoviruses constructed with Red-Green-HIV (RGH) backbone and envelope from HxB2 (X4-tropic) and JR-FL (R5-tropic) were used to infect PB-CD34 cells. (a) Schematic representation for active infection indicated by GFP fluorescence (green), integrated viral DNA (latency) by mCherry fluorescence (pink), and active replication from integrated genome (yellow). (b) Fluorescence microscopy was used to examine eGFP and mCherry signals 2 days after infection of GHOST(3)-CXCR4$^+$CCR5$^+$ cells. (c) PB-CD34 cells were infected with X4-RGH or R5-RGH virus for 24 hours and examined under confocal microscopy with blue signals depicting Hosecht DNA/nucleus stain. (d) Results from independent experiments.

R5-RGH viruses had mainly red signals (Fig 2c, 2d), suggesting that latent infections were established by the pseudovirus, albeit a low level of subsequent replication. However, for R5-RGH, a slight but significant increase in active infection was observed and most cells still retained HIV-1 latency (Fig 2c, 2d). Therefore, using the dual-reporter pseudovirus system, CD34+ cells can be successfully infected with characteristic of integration and replication and confirms that CD34+ cells can be infected by HIV-1.

HIV-1 can transmit from infected PB-CD34 cells to autologous CD4+ T cells

HIV-1–infected PB-CD34 cells were shown to be capable of eliciting an immune response by upregulation of type I IFNs and MHC-I/II molecules. We then sought to determine if HIV-1 transmission can occur to CD4+ T cells. First, PB-CD34 cells were mock or infected by HIV-1NL4-3 for 7 days. By day 6, naive CD4+ T cells were isolated from the same donor PBMCs using magnetic beads, and left in media or stimulated with PHA or anti-CD3/anti-CD28 antibodies for 24 hours. To note, ELISA did not detect any p24 in the supernatant of PB-CD34 cells at day 7 post-infection. On day 7, co-culture occurred at a ratio of one PB-CD34 cell to five CD4+ T cells. One day later, cells were subjected to intracellular immunostaining for p24 following surface CD34, CD4, and activation marker CD25 staining, and analysed by flow cytometry. Following gating on CD34- cells, CD4 cells were analysed for p24 signals among CD25+ and CD25- cells. Following co-culture, p24 signals can be detected in naive CD4+ T cells without stimulation but upregulated for CD25 (Fig 3). PHA or anti-CD3/anti-CD28 stimulated cells did not display p24+ cells. This is in stark contrast to HIV-1–free virus infection of CD4+ T cells where activated cells are required for efficient infection. When a transwell was used to separate PB-CD34 cells and CD4+ T cells, no viral p24 signals was detected on CD4+ T cells (data not shown), suggesting that direct cell-cell contact is required for viral transmission. Interestingly, the up-regulation of CD25 following co-culture among naive CD4+ T cells suggest that upon interaction with infected PB-CD34 cells, the naive T cells are activated in a certain level, probably due to the unregulated type I IFNs and MHC-I/II antigen presentation molecules.

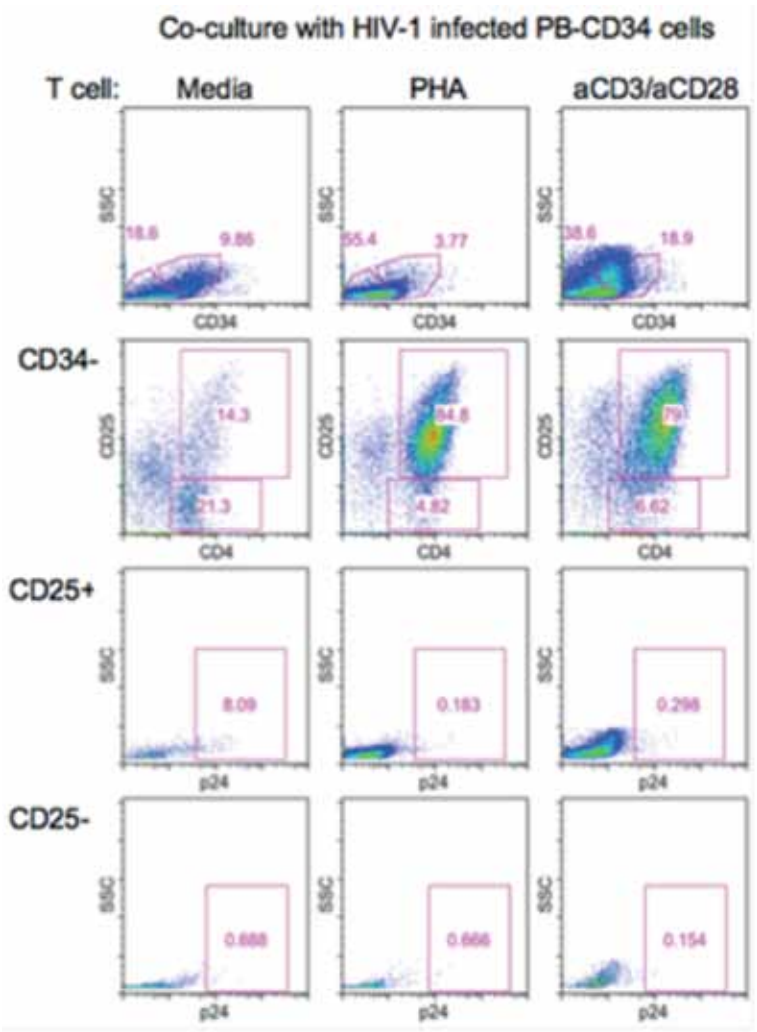

FIG 3. Cell-cell transmission of HIV-1 from infected PB-CD34 cells to autologous CD4+ T cells: PB-CD34 cells were infected for 7 days before co-culture with naive CD4+ T cells unstimulated or stimulated with PHA (5 μg/mL) or anti-CD3/anti-CD28 antibodies (0.5 μg/mL) for another 24 hours. Representative flow cytometry plots showing gating strategy to analyse p24 signals among CD25+ or CD25- subsets in CD34-CD4+ cells.

Discussion

Infection of CD34+ cells by HIV-1 remains controversial in two aspects: (1) whether CD34+ cells can be infected by HIV-1, and (2) whether a latent reservoir is established. The difficulty of addressing these issues mainly lie at the lack of a robust cell-based model of study. Thus, this study provided a robust peripheral blood-derived CD34+ cell culture model that can support HIV-1 infection, integration, and replication, and a mean of viral transmission by cell-cell spread to CD4+ T cells.

The importance of CD34+ cells as a latent reservoir has been neglected. We showed that CD34+ cells can act as effectors of innate immune response through expression of PRRs and inducible type I IFNs, as well as expression of antigen presenting MHC-I/II molecules. Notwithstanding that the HSCs infected by HIV-1 have a higher tendency towards the myeloid lineage likely due to recognition of HIV-1. HIV-1 could be transmitted through cell-cell contact; these cells along with dendritic cells and macrophages contribute to CD4+ T cell depletion. However, whether this occurs in the bone marrow or the periphery remains to be investigated.

Acknowledgements

This study was supported by the Health and Medical Research Fund, Food and Health Bureau, Hong Kong SAR Government (#13120612). We thank Miss Yiru Huang, Ms Hau-yee Kwok, Dr Min Chen, Mr Lijun Ling.

References

1. Shan L, Deng K, Shroff NS, et al. Stimulation of HIV-1-specific cytolytic T lymphocytes facilitates elimination of latent viral reservoir after virus reactivation. Immunity 2012;36:491-501.
2. Buzon MJ, Sun H, Li C, et al. HIV-1 persistence in CD4+ T cells with stem cell-like properties. Nat Med 2014;20:139-42.
3. Redel L, Le Douce V, Cherrier T, et al. HIV-1 regulation of latency in the monocyte-macrophage lineage and in CD4+ T lymphocytes. J Leukoc Biol 2010;87:575-88.
4. Carter CC, Onafuwa-Nuga A, McNamara LA, et al. HIV-1 infects multipotent progenitor cells causing cell death and establishing latent cellular reservoirs. Nat Med 2010;16:446-51.
5. Malnati MS, Scarlatti G, Gatto F, et al. A universal real-time PCR assay for the quantification of group-M HIV-1 proviral load. Nat Protoc 2008;3:1240-8.

Foreign language learning as potential treatment for mild cognitive impairment

PCM Wong *, J Ou, CWY Pang, L Zhang, CS Tse, LCW Lam, M Antoniou

KEY MESSAGES

1. Improvement in cognitive abilities can be achieved in older adults with mild cognitive impairment.
2. Cognitively stimulating activities, including foreign language learning, is a potentially effective intervention.

Hong Kong Med J 2019;25(Suppl 7):S41-3
HMRF project number: 01120616

[1,2,3] **PCM Wong,** [1,2] **J Ou,** [1,2] **CWY Pang,** [4] **L Zhang,** [5] **CS Tse,** [6] **LCW Lam,** [7] **M Antoniou**

[1] *Department of Linguistics and Modern Languages, The Chinese University of Hong Kong, China*
[2] *Brain and Mind Institute, The Chinese University of Hong Kong, China*
[3] *Department of Otorhinolaryngology, Head and Neck Surgery, The Chinese University of Hong Kong, China*
[4] *Department of Chinese Language Studies, The Education University of Hong Kong, China*
[5] *Department of Educational Psychology, The Chinese University of Hong Kong, China*
[6] *Department of Psychiatry, The Chinese University of Hong Kong, China*
[7] *The MARCS Institute for Brain, Behaviour and Development, Western Sydney University, Australia*

* Principal applicant and corresponding author: p.wong@cuhk.edu.hk

Introduction

As the number of older adults increases, age-related health issues (both physical and cognitive) and associated costs are expected to increase, placing emotional and financial stress on family members and the health system. Dementia is one of the most devastating and costly diseases that older adults face. The present study aimed to determine whether foreign language learning can improve cognitive outcomes of older adults with mild cognitive impairment (MCI). The objectives are to determine whether foreign language learning is (1) effective in boosting cognitive reserve and promoting healthy cognitive function and (2) superior to other established cognitively stimulating activities such as crossword and logic puzzles.

Methods

All participants gave written informed consent in accordance with the protocol approved by the Joint Chinese University of Hong Kong – New Territories East Cluster Clinical Research Ethics Committee. Participants were Cantonese speakers with minimal exposure to English. Of 137 participants with MCI enrolled, 86 (mean age, 71.8±6.3 years) completed all phases of the study. MCI was defined as a score of 0.5 on the Clinical Dementia Rating (CDR) or a score of 0 on the CDR plus 1.5 standard deviations below the age-typical mean on the Chinese version of the Alzheimer's Disease Assessment Scale—Cognitive subscale (ADAS-Cog) or the Category Verbal Fluency Test (CVFT). The latter criterion was designed to capture older adults who may score normal on the CDR but show subtle deficits in neuropsychological measures.

Participants were randomly assigned to one of three groups: experimental group (n=29) who completed levels 1-5 of the Rosetta Stone English language training software (that uses a combination of images, text, and sounds to teach vocabulary and grammar in a way designed to simulate immersion learning), active control group (n=29) who completed computer-delivered crossword and logic puzzles, and passive control group (n=28) who listened to and read about the background of Chinese music through a computer. Participants in the three groups were closely matched in age ($F(2, 85)=0.41$, P=0.67) and years of education ($F(2, 85)=1.29$, P=0.28).

Participants were familiarised with the computer software interface at the onset of training. The training was up to 5 hours per week for 6 months. In addition, each group met for occasional social activities led by the research assistant or social group leader: the experimental group practised English skills with an English speaker; the active control group played games in a group setting (eg Pictionary); and the passive control group discussed music or sang.

Cognitive outcome was measured at the start of training (pretest), at the end of training at 12 months (posttest), and at 3 months after the end of training (follow-up) using the Auditory Reading Span, the Simon Task, Wechsler Digit Span, the Boston

TABLE. Cognitive outcome by group across three time points*

Cognitive outcome	Experimental group (n=29)			Active control group (n=29)			Passive control group (n=28)		
	Pretest	Posttest	Follow-up	Pretest	Posttest	Follow-up	Pretest	Posttest	Follow-up
Clinical Dementia Rating (total score range, 0-3)	0.39±0.21	0.28±0.25	0.31±0.25	0.39± 0.21	0.29±0.25	0.29±0.25	0.37±0.22	0.25±0.25	0.28±0.25
Alzheimer's Disease Assessment Scale–Cognitive subscale (total score range, 0-70)	11.53±3.55	7.43±4.08	6.91±2.79	12.45±4.85	8.70±4.74	9.01±4.85	12.55±4.88	10.66±6.03	9.62±5.76
Category Verbal Fluency Test (total score range, 0-66)	40.48±10.66	41.38±10.36	42.31±9.87	37.72±9.20	39.72± 9.90	40.24±12.33	36.57±7.24	36.75±8.73	36.96±7.78

* Data are presented as mean ± standard deviation

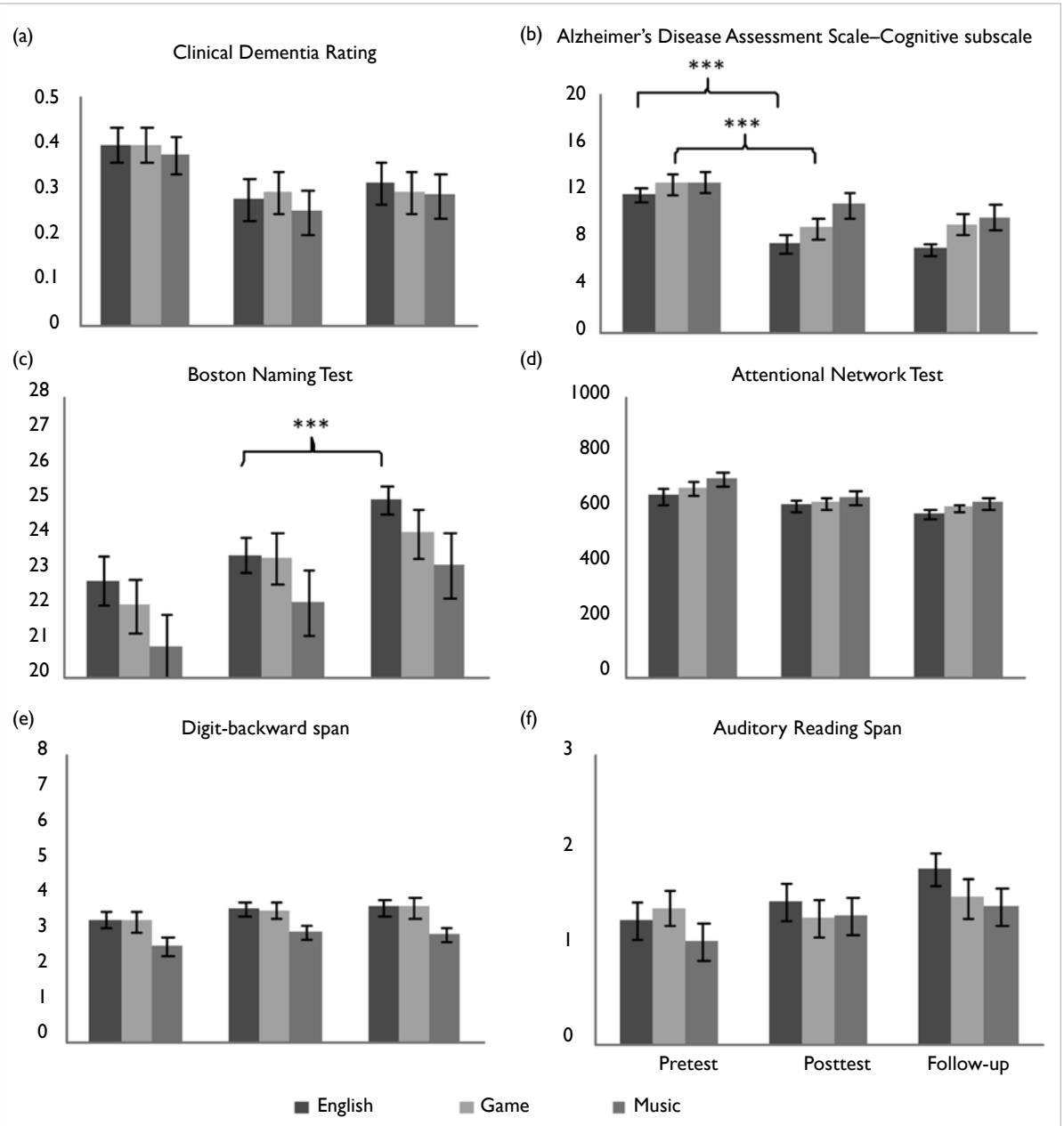

FIG. Cognitive outcome measures at three time points: (a) Clinical Dementia Rating, (b) Alzheimer's Disease Assessment Scale–Cognitive subscale, (c) Boston Naming Test, (d) Attentional Network Test, (e) digit-backward span, and (f) Auditory Reading Span.

Naming Test, and the Attention Network Test. Cognitive function, attention, and working memory are sensitive to age-related cognitive decline.

A 3x3 repeated measures ANOVA of the three groups and three time points was used. Planned comparisons were made using t-tests.

Results

The three groups were comparable at pre-test (Table). Across groups, significant main effects of time were found for CDR [$F(2, 166)=8.1$, $P<0.0001$, $\eta^2=0.089$], ADAS-Cog [$F(2, 166)=38.3$, $P<0.0001$, $\eta^2=0.316$], Boston Naming Test [$F(2, 166)=31.5$, $P<0.0001$, $\eta^2=0.275$], Attention Network Test [$F(2, 166)=9.4$, $P<0.0001$, $\eta2=0.102$], digit-backward span [$F(2, 83)=6.3$, $P=0.002$, $\eta^2=0.070$], and Auditory Reading Span [$F(2, 166)=4.2$, $P=0.016$, $\eta^2=0.049$] (Fig). However, Auditory Reading Span did not pass the correction for multiple comparisons (at $P<0.005$). CDR, ADAS-Cog, Attention Network Test, and digit-backward span improved significantly from pretest to posttest ($P<0.013$), but scores remaining stable from posttest to follow-up ($P>0.05$). Only the Boston Naming Test score improved significantly at both posttest ($P<0.001$) and follow-up ($P<0.001$).

There were no significant effects of group ($P>0.09$) or group-by-time interactions ($P>0.11$). However, foreign language learning produced significant improvement in ADAS-Cog and Boston Naming Test scores after Bonferroni correction for family-wise type 1 error at $P<0.005$. Specifically, the experimental group achieved significant improvement in ADAS-Cog from pretest to posttest [$t(28)= -6.02$, $P<0.0001$, Cohen's $d= -1.07$] and in Boston Naming Test from pretest to follow-up [$t(28)=4.59$, $P<0.0001$, Cohen's $d=0.639$]. Compared with the experimental group, the passive control group only achieved improvements in CDR ($P=0.02$) and Attention Network Test ($P=0.01$) from pretest to posttest, but these effects did not pass Bonferroni correction. Thus, foreign language training was more effective than music listening in boosting cognitive reserve and promoting healthy cognitive function. Compared with the experimental group, the active control group only achieved improvement in ADAS-Cog [$t(28)= -4.58$, $P<0.0001$, Cohen's $d= -0.778$] from pretest to posttest. Thus, foreign language training was more effective than crossword and puzzles in reducing the risk of cognitive deficits and in improving a broader range of cognitive functions. Attention Network Test and digit-backward span was not significant in any of the three groups ($P>0.07$).

Discussion

As far as we are aware, this is the first prospective, randomised control study to evaluate foreign language learning on cognitive improvement in older adults with MCI. The protective effect of bilingualism on cognitive decline in older adults has been reported.[4] However, those studies were retrospective in nature and lifelong bilingualism was the focus. In the present study, we demonstrated that both short-term learning of a new language and other active cognitively stimulating activities could enhance cognitive functions. Nonetheless, the effect of foreign language learning was larger on ADAS-Cog. In addition, the training-induced benefit in the cognitive measure of linguistic function was only observed in the experimental group.

Acknowledgements

This study was supported by the Health and Medical Research Fund, Food and Health Bureau, Hong Kong SAR Government (#01120616). We thank our collaborating community centres for their support.

Results from this study have been published in: Wong PCM, Ou J, Pang CWY, et al. Language training leads to global cognitive improvement in older adults: a preliminary study. J Speech Lang Hear Res 2019;62:2411-24. (https://pubs.asha.org/doi/10.1044/2019_JSLHR-L-18-0321)

References

1. Antoniou M, Gunasekera GM, Wong PC. Foreign language training as cognitive therapy for age-related cognitive decline: a hypothesis for future research. Neurosci Biobehav Rev 2013;37:2689-98.
2. Selkoe DJ. Preventing Alzheimer's disease. Science 2012;337:1488-92.
3. Lam LC, Tam CW, Lui VW, et al. Prevalence of very mild and mild dementia in community-dwelling older Chinese people in Hong Kong. Int Psychogeriatr 2008;20:135-48.
4. Bialystok E, Craik FI, Freedman M. Bilingualism as a protection against the onset of symptoms of dementia. Neuropsychologia 2007;45:459-64.

FE65 serine-610 phosphorylation and its functional implications in Alzheimer disease amyloid precursor protein processing

KF Lau *, WN Chow, JCK Ngo, YW Chen, VKM Tam, EHY Chan, C Miller

KEY MESSAGES

1. FE65 Serine610 (S610) phosphorylation regulates amyloid precursor protein (APP)/FE65 interaction and FE65-mediated APP processing.
2. FE65 S610 is phosphorylated by serum- and glucocorticoid-induced kinase 1.
3. The effect of FE65 S610 phosphorylation on APP processing is associated with the role of FE65 in metabolic turnover of APP via the proteasome.

Hong Kong Med J 2019;25(Suppl 7):S44-7
HMRF project number: 01120196

[1] KF Lau, [1] WN Chow, [1] JCK Ngo, [2] YW Chen, [1] VKM Tam, [1] EHY Chan, [3] C Miller

[1] *School of Life Sciences, The Chinese University of Hong Kong*
[2] *Randall Division of Cell and Molecular Biophysis, King's College London*
[3] *Basic and Clinical Neuroscience, King's College London*

* Principal applicant and corresponding author: kflau@cuhk.edu.hk

Introduction

Aggregation of amyloid-β peptide (Aβ), derived from the aberrant processing of amyloid precursor protein (APP), is crucial in the pathogenesis of Alzheimer disease. FE65 is a neural enriched adaptor protein that interacts with APP via its PTB1 domain. FE65/APP interaction can stimulate APP processing. Therefore, it is essential to understand the mechanism(s) by which FE65/APP interaction is regulated. FE65 is a phospho-protein with several reported phosphorylation sites. However, the biological significance of FE65 phosphorylation is largely unknown. FE65 Serine-610 (S610) is an uncharacterised phospho-residue located in the interaction interface of APP/FE65. Phosphorylation of FE65 S610 may play a role in regulating APP/FE65 interaction and altering APP processing.

Methods

Phosphomimetic mutants in GST pull down and co-immunoprecipitation assays were used to determine the effect of FE65 S610 phosphorylation on APP/FE65 interaction. APP processing was determined by APP-GAL4 luciferase reporter assay, APP C-terminal fragment analysis, and Aβ ELISA. FE65 S610 kinase was identified by Kinase Finder radiometric protein kinase assays and then validated by in vitro and in vivo kinase assays. The effect of FE65 on APP protein turnover was analysed by cycloheximide chase assay.

Results

Phosphorylation of FE65 S610 interferes with APP-FE65 interaction

According to the crystal structure of AICD/FE65-PTB2 complex, FE65 S610 is found to lie in their interaction interface. Such residue is phosphorylated in an FE65 isoform from mass spectrometric analysis. To test whether FE65 S610 phosphorylation alters APP/FE65 interaction, co-immunoprecipitation was performed by co-transfecting APP with either myc-tagged FE65 S610A or S610D to CHO cells. Western blotting revealed that greater amount of APP co-immunoprecipitated with FE65 S610A than with FE65 S610D (Fig 1). This evidence suggested that phosphorylation of FE65 S610 attenuates APP-FE65 interaction.

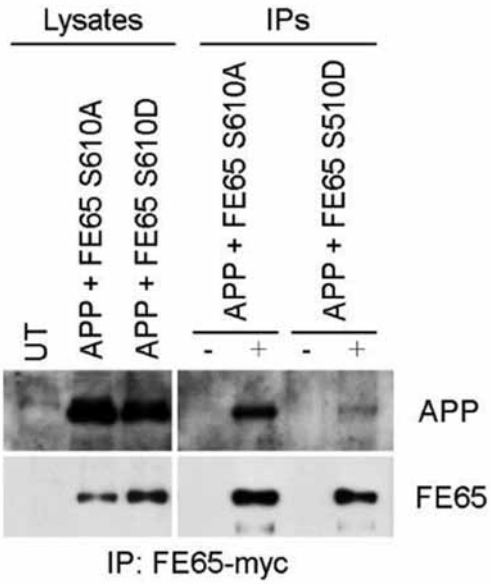

FIG 1. FE65 S610 phosphomimetic mutation reduces amyloid precursor protein (APP)/FE65 interaction. Bacterially expressed GST-APPc was used as bait for GST pull-down assay from FE65 S610A- or S610D-transfected cell lysate. FE65 S610A and S610D were detected by 9B11 anti-myc antibody against the C-terminal myc tag.

SGK1 phosphorylates FE65 S610

To identify FE65 S610 kinases, we used commercial Kinase Finder radiometric protein kinase assay (ProQinase, Germany), which is a radiometric kinase assay for a panel of 190 serine/threonine kinases. The results suggested that SGK1 is a putative FE65 S610 kinase (data not shown). Intriguingly, the amino acid sequence around FE65 S610 is found to be SGK1 targeting consensus (R-X-R-X-X-S/T-φ; φ = hydrophobic residue).[1,2] In order to validate FE65 S610 as the target residue of SGK1, bacterially expressed GST-FE65598-619 WT and GST-FE65598-619 S610A were incubated with SGK1-CA immunoprecipitated from transfected cell lysate together with [γ-^{32}P]-ATP for 30 minutes at 30°C. The reaction mixture was resolved on SDS-PAGE and exposed to an autoradiogram. SGK1 induced phosphorylation on wildtype but not on S610A mutant (Fig 2a).

To determine whether SGK1 interferes with APP-FE65 interaction, co-immunoprecipitation was performed from cells co-transfected with APP + FE65 or APP + FE65 + SGK1-CA. FE65 was immunoprecipitated by an anti-myc antibody and the immunocomplex was detected for APP. Less APP co- immunoprecipitated with FE65 in the presence of SGK1-CA, indicating that SGK1-CA weakens the interaction between APP and FE65 (Fig 2b).

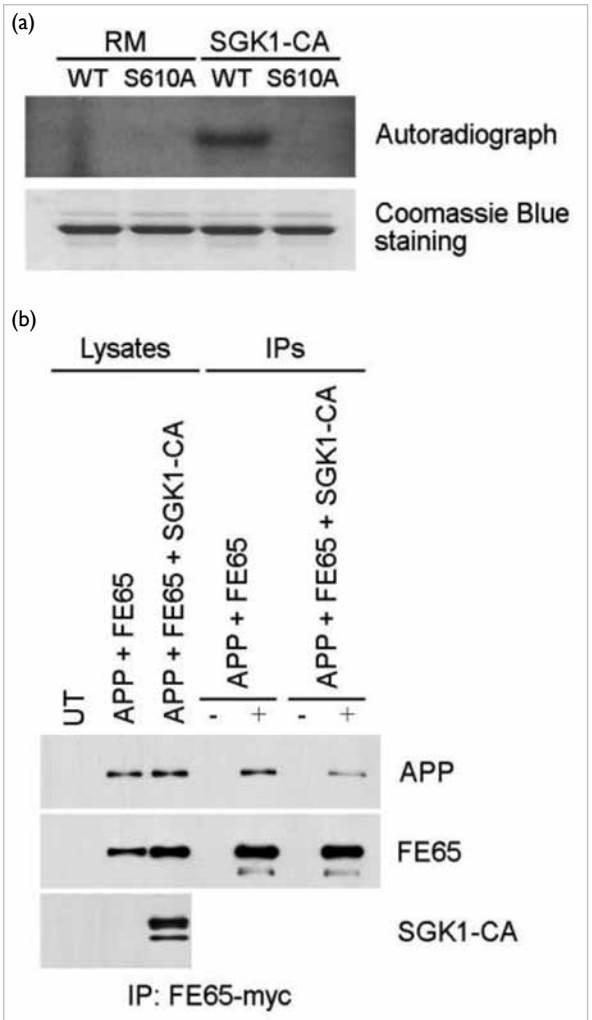

FIG 2. SGK1 phosphorylates FE65 S610 and to reduces amyloid precursor protein (APP)/FE65 interaction. (a) Bacterially expressed GST-FE65598-619 WT or S610A were incubated with SGK1-CA immunoprecipitated from transfected cell lysate together with [γ-32P]-ATP for 30 minutes at 30°C. RM is the reaction mix only without kinase. (b) Co-immunoprecipitation was performed from CHO cells transfected with APP + FE65 or APP + FE65 + SGK1-CA using anti-myc antibody. APP was detected with anti-APP antibody while FE65 was detected by an anti-myc antibody. SGK1 interferes with APP/FE65 interaction.

Phosphorylation of FE65 S610 abolishes the effect of FE65 on Aβ generation by enhancing APP degradation via proteasome

Aberrant processing of APP results in excessive Aβ generation, and the process is known to be modulated by a number of APP-interacting proteins including FE65. As FE65 S610 phosphorylation prevents APP-FE65 interaction, we speculated that this phosphorylation event might be involved in the regulation of FE65-mediated APP processing. APP + FE65/FE65 S610A/FE65 S610D were co-transfected into CHO cells, and the amount of secreted Aβ was measured by Aβ ELISA kit. The amount of Aβ was elevated in cells overexpressing FE65 or FE65 S610A but not in cells overexpressing FE65 S610D (Fig 3a). SGK1-CA suppressed FE65-mediated increase in Aβ generation but had no significant effect on FE65 S610A-promoted Aβ level (Fig 3b). This finding further supports that phosphorylation of FE65 at S610 by SGK1 abolishes the effect of FE65 on APP processing and Aβ generation.

To determine the effect of FE65 S610 phosphorylation on the turnover of APP, APP knockdown resulted in reduction of FE65 and FE65 S610A levels (lane 1 vs lane 2; lane 5 vs lane 6), and the depletion was blocked upon proteasome inhibitor MG132 treatment (lane 3 vs lane 4; lane 7 vs lane 8) [Fig 3c]. This indicates that APP stabilises FE65 and FE65 S610A by preventing their degradation through Ubiquitin-Proteasome System (UPS). Nonetheless, the protein level of FE65 S610D, which is unable to bind to APP, was not affected by endogenous APP level (lane 9 vs lane 10). Taken together, the current findings suggest that the interaction between APP and FE65 protects both APP and FE65 from being degraded through UPS, and this process is regulated by the phosphorylation status of FE65 S610.

Discussion

We demonstrated that phosphorylation of FE65 S610 by SGK1 attenuates the interaction between

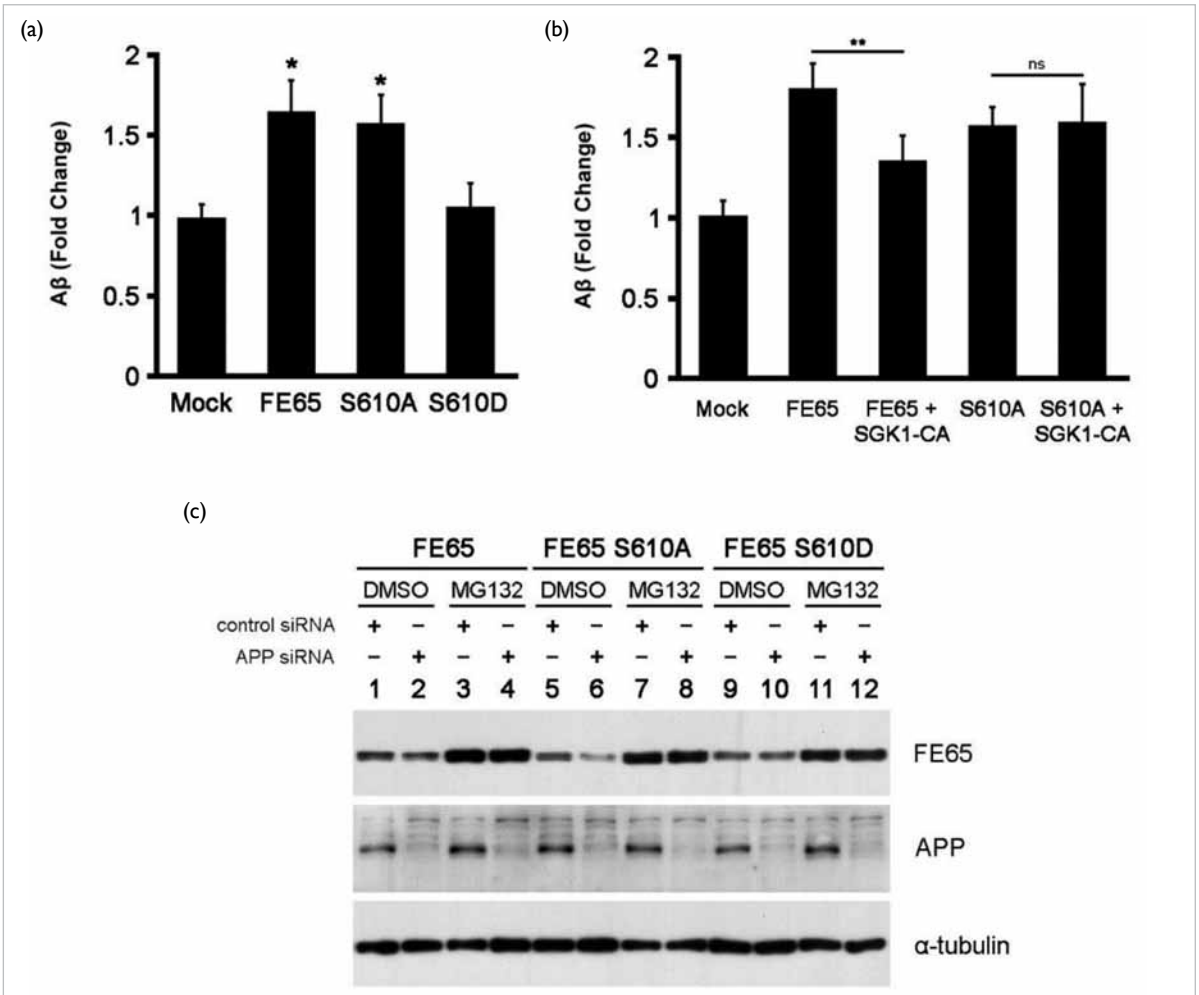

FIG 3. Phosphorylation of FE65 S610 and abolishes the effect of FE65 on Aβ generation by enhancing amyloid precursor protein (APP) degradation via proteasome. (a) CHO cells were co-transfected with APP + mock, FE65, FE65 S610A or FE65 S610D. At 48 hours post-transfection, cell culture medium were aspirated and changed to fresh medium. The level of secreted **Aβ** was assayed using ELISA kit 7 hours after change of medium. FE65 S610D does not enhance **Aβ** liberation. (b) CHO cells were co-transfected with APP + the indicated constructs, and the level of secreted **Aβ** was assayed. SGK1 suppresses FE65-enhanced **Aβ** liberation through phosphorylation of S610. (c) Cells co-transfected with FE65, FE65 S610A, or FE65 S610D + control or APP siRNA were incubated with 2.5 μM MG132 or DMSO vehicle for 16 hours. The protein levels of FE65 in transfected cell lysates were compared by western blotting. APP knockdown-mediated reduction of FE65 and FE65 S610A levels is rescued by MG132. Protein level of FE65 S610D is unaffected by APP knockdown.

FE65 and APP. Our findings are similar to those of others who provided evidence that SGK1 phosphorylates a rat variant of FE65.[3] FE65 S610 is located within the PTB2 domain of FE65, which is the domain that is responsible for APP binding. In fact, structural analysis of FE65 PTB2 domain in complex with AICD revealed that S610 is involved in the interaction interface. Our experimental data and molecular dynamics simulation further support the importance of FE65 S610 as a critical amino acid in APP-FE65 interaction and reveals a novel molecular mechanism that modulates APP-FE65 interaction.

Regulation of APP holoprotein level is important for AD pathogenesis. First, triplication of APP gene on chromosome 21 in patients with Down syndrome is associated with development of early onset AD. On the contrary, in patients with Down syndrome with only partial trisomy 21 that excludes APP gene, AD pathology was not observed even at advanced age. Second, APP mRNA level was reported to be elevated in sporadic AD, accompanied by a marked decrease in miR-106b, a negative regulator of APP expression. Third, degradation of APP through lysosomal pathway and proteasomal pathway has been implicated in reduction of Aβ liberation. We showed that FE65 stabilises APP holoprotein and prolongs its half-life by preventing APP degradation through UPS. Previously, we had demonstrated that FE65 stabilises p53 and huntingtin (Htt) by suppressing their degradation through UPS.[4] The

current finding has two important implications: (1) it reinforces the role of FE65 as a negative regulator in UPS-mediated degradation, and (2) FE65 serves to suppress APP holoprotein turnover through UPS, thereby enhancing Aβ generation, in addition to acting as a bridging molecule between APP and ApoE receptors such as LRP1, ApoER2, and VLDLR which modulate APP processing.

APP can be targeted to proteasome through multiple pathways. For instance, APP was reported to be an ER-associated degradation substrate where it is ubiquitinated by ER-localised E3 ubiquitin ligase HRD1, and the stress-responsive chaperone-protease HtrA2, through binding to the N-terminal region of APP, serves as a shuttling chaperone to assist proteasome targeting. Alternatively, APP can be ubiquitinated by the F-box and leucine rich repeat protein 2, a component of the SCF (Skp1-Cullin1-F-box protein) E3 ubiquitin ligase complex, resulting in enhanced proteasomal degradation. Of note, Aβ generation was reported to decrease by the aforementioned pathways. It is therefore possible that FE65 inhibits APP proteasomal degradation by competing with the E3 ubiquitin ligases HRD1 and F-box and leucine rich repeat protein 2 for APP binding, thereby promoting Aβ generation. Further investigation on the underlying mechanism by which FE65 blocks APP degradation through UPS is warranted.

The phosphorylation status of FE65 S610 was shown to regulate the turnover rate of APP. Consistent with the interaction behaviour, phosphorylation of FE65 S610 abrogates the stabilisation effect on APP, leading to a shorter half-life. This provides a mechanistic explanation to the regulatory effect of FE65 S610 phosphorylation on APP processing. Additionally, we provided evidence that degradation of FE65 and FE65 S610A through UPS is suppressed by APP, a phenomenon which is not observed in FE65 S610D. Our current finding underscores the importance of APP-FE65 interaction in regulating the turnover of both APP and FE65 through UPS, which in turn modulates APP processing and thus Aβ generation.

Furthermore, we demonstrated that SGK1 attenuates APP-FE65 interaction through FE65 S610 phosphorylation and suppresses FE65-enhanced Aβ secretion. SGK1 is a serine/threonine kinase downstream of the phosphatidylinositol 3-kinase (PI3K) cascade and its expression is acutely regulated by serum and glucocorticoids. SGK1 has been shown to phosphorylate the γ-secretase component Nicastrin and promote its degradation. Examination of APP, C-terminal fragment, and AICD protein levels and activity of C99-GAL4/VP16 luciferase reporter revealed that γ-secretase-mediated APP cleavage is suppressed by SGK1. Our work demonstrated that SGK1, through phosphorylating FE65 S610, modulates Aβ liberation and that a novel pathway by which SGK1 regulates APP processing.

Acknowledgements

This study was supported by the Health and Medical Research Fund, Food and Health Bureau, Hong Kong SAR Government (#01120196) and CUHK direct grant scheme. We thank David Pearce for mammalian expression SGK1 construct.

Results from this study have been published in:

(1) Chow WN, Ngo JCK, Li W, et al. Phosphorylation of FE65 Ser610 by serum- and glucocorticoid-induced kinase 1 modulates Alzheimer's disease amyloid precursor protein processing. Biochem J 2015;470:303-17.

(2) Chow WN, Cheung HN, Li W, Lau KF. FE65: roles beyond amyloid precursor protein processing. Cell Mol Biol Lett 2015;20:66-87.

References

1. Haass C, Kaether C, Thinakaran G, Sisodia S. Trafficking and proteolytic processing of APP. Cold Spring Harb Perspect Med 2012;2:a006270.
2. Standen CL, Brownlees J, Grierson AJ, et al. Phosphorylation of thr(668) in the cytoplasmic domain of the Alzheimer's disease amyloid precursor protein by stress-activated protein kinase 1b (Jun N-terminal kinase-3). J Neurochem 2001;76:316-20.
3. McLoughlin DM, Miller CC. The FE65 proteins and Alzheimer's disease. J Neurosci Res 2008;86:744-54.
4. Chow WN, Luk HW, Chan HY, Lau KF. Degradation of mutant huntingtin via the ubiquitin/proteasome system is modulated by FE65. Biochem J 2012;443:681-9.

Published by the Hong Kong Academy of Medicine Press for the Government of the Hong Kong Special Administrative Region. The opinions expressed in the *Hong Kong Medical Journal* and its supplements are those of the authors and do not reflect the official policies of the Hong Kong Academy of Medicine, the Hong Kong Medical Association, the institutions to which the authors are affiliated, or those of the publisher.